



Published in final edited form as:

Cell Rep. 2022 September 06; 40(10): 111306. doi:10.1016/j.celrep.2022.111306.

Genetic- and diet-induced ω -3 fatty acid enrichment enhances TRPV4-mediated vasodilation in mice

Rebeca Caires¹, Tessa A.C. Garrud¹, Luis O. Romero^{1,2}, Carlos Fernández-Peña^{1,3}, Valeria Vásquez¹, Jonathan H. Jaggar¹, Julio F. Cordero-Morales^{1,4,*}

¹Department of Physiology, College of Medicine, University of Tennessee Health Science Center, Memphis, TN 38163, USA

²Integrated Biomedical Sciences Graduate Program, College of Graduate Health Sciences, Memphis, TN 38163, USA

³Present address: St. Jude Children's Research Hospital, Memphis, TN 38105, USA

⁴Lead contact

SUMMARY

TRPV4 channel activation in endothelial cells leads to vasodilation, while impairment of TRPV4 activity is implicated in vascular dysfunction. Strategies that increase TRPV4 activity could enhance vasodilation and ameliorate vascular disorders. Here, we show that supplementation with eicosapentaenoic acid (EPA), an ω -3 polyunsaturated fatty acid known to have beneficial cardiovascular effects, increases TRPV4 activity in human endothelial cells of various vascular beds. Mice carrying the *C. elegans* FAT-1 enzyme, which converts ω -6 to ω -3 polyunsaturated fatty acids, display higher EPA content and increased TRPV4-mediated vasodilation in mesenteric arteries. Likewise, mice fed an EPA-enriched diet exhibit enhanced and prolonged TRPV4-dependent vasodilation in an endothelial cell-specific manner. We also show that EPA supplementation reduces TRPV4 desensitization, which contributes to the prolonged vasodilation. Neutralization of positive charges in the TRPV4 N terminus impairs the effect of EPA on channel desensitization. These findings highlight the beneficial effects of manipulating fatty acid content to enhance TRPV4-mediated vasodilation.

Graphical abstract

This is an open access article under the CC BY-NC-ND license (<http://creativecommons.org/licenses/by-nc-nd/4.0/>).

*Correspondence: jcordero@uthsc.edu.

AUTHOR CONTRIBUTIONS

Lead author, J.F.C.-M.; conceptualization, V.V. and J.F.C.-M.; methodology, V.V., J.H.J., and J.F.C.-M.; formal analysis and investigation, R.C., T.A.C.G., L.O.R., V.V., and C.F.-P.; writing – original draft preparation, R.C., V.V., and J.F.C.-M.; writing – review & editing, V.V., J.H.J., and J.F.C.-M.; supervision, V.V., J.H.J., and J.F.C.-M.; project administration, J.F.C.-M.; funding acquisition, V.V., J.H.J., and J.F.C.-M.

SUPPLEMENTAL INFORMATION

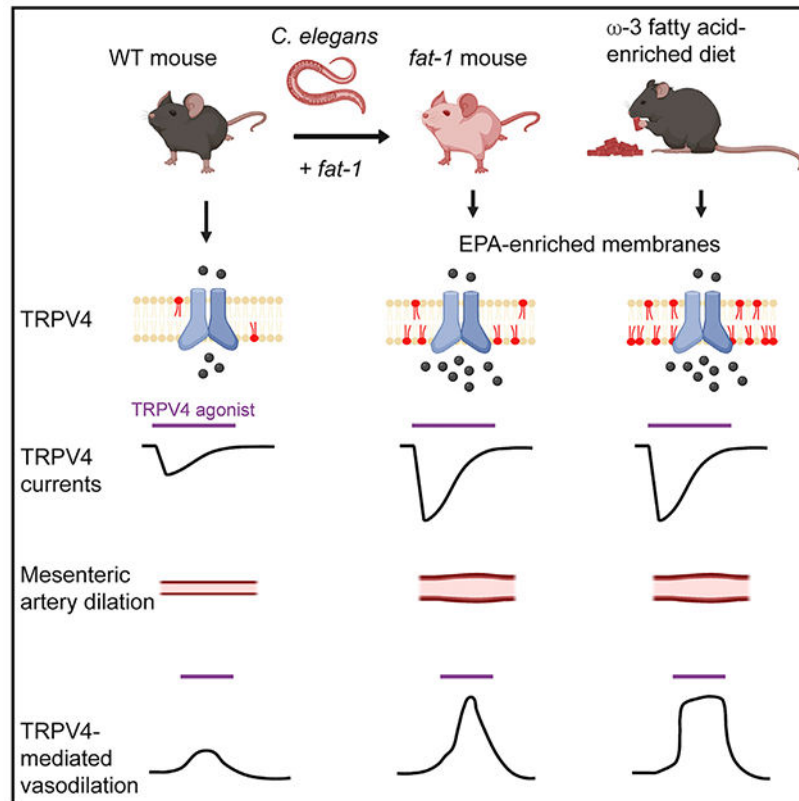
Supplemental information can be found online at <https://doi.org/10.1016/j.celrep.2022.111306>.

DECLARATION OF INTERESTS

The authors declare no competing interests.

INCLUSION AND DIVERSITY

One or more of the authors of this paper self-identifies as an underrepresented ethnic minority in science.



In brief

Reduced TRPV4 activity is associated with vascular dysfunction. Dietary consumption of ω -3 fatty acids, present in fish oils, is known to have beneficial cardiovascular effects. Caires et al. show that genetic or dietary enrichment of an ω -3 fatty acid enhances TRPV4 function in endothelial cells and TRPV4-mediated vasodilation in mice.

INTRODUCTION

The transient receptor potential vanilloid 4 (TRPV4) is a polymodal cation channel that is activated by mild temperatures and chemical ligands, as well as downstream of osmolarity changes and shear stress (Hartmannsgruber et al., 2007; Liedtke et al., 2000; Strotmann et al., 2000; Thorneloe et al., 2008; Vriens et al., 2004; Watanabe et al., 2002a, 2002b; Wissenbach et al., 2000). TRPV4 is expressed in a variety of vascular beds, including endothelial cells of large (conduit) arteries and small (resistance size) arterioles, where it plays a crucial role in regulating vascular tone and blood flow (Alvarez et al., 2006; Earley et al., 2009; Filosa et al., 2013; Kohler et al., 2006; Vriens et al., 2005; Watanabe et al., 2002a; Willette et al., 2008). TRPV4 enables endothelial cells, smooth muscle cells, and perivascular neurons to integrate hemodynamic forces to regulate systemic blood pressure (Peixoto-Neves et al., 2015; Sonkusare et al., 2012; White et al., 2016). Activation of TRPV4 leads to an increase in intracellular calcium (Ca^{2+}) concentration, followed by the activation of small (SK)- and intermediate (IK)-conductance Ca^{2+} -activated potassium

channels and nitric oxide synthase, with subsequent smooth muscle cell hyperpolarization and vasodilation (Earley et al., 2005, 2009; Kohler et al., 2006; Sonkusare et al., 2012).

Changes in TRPV4 expression and activity are associated with various vascular pathologies (Baylie and Brayden, 2011; Grace et al., 2017; White et al., 2016). For instance, impairment of TRPV4 function in endothelial cells contributes to obesity-induced hypertension (Ottolini et al., 2020). Downregulation of TRPV4 impairs endothelium-dependent hyperpolarization in mesenteric arteries of stroke-prone spontaneously hypertensive rats (Seki et al., 2017). It has also been suggested that TRPV4 downregulation by hyperglycemia and diabetes is associated with endothelial dysfunction and retinopathy (Monaghan et al., 2015). Moreover, reduced flow-mediated vasodilation in mesenteric arteries of aged rats was restored after increasing TRPV4 expression (Du et al., 2016). Likewise, activation of TRPV4 by plant-derived molecules increases vasodilation in mesenteric arteries, suggesting that channel modulation may aid in the regulation of local blood flow (Ma et al., 2012; Peixoto-Neves et al., 2015; Zhang et al., 2019). Together, these studies support the notion that TRPV4 is essential for proper vascular function and suggest that increasing TRPV4 expression and/or activity may ameliorate vascular disorders.

Polyunsaturated fatty acids (PUFAs) and their derivatives are among the membrane lipid components that regulate ion channel function (Caires et al., 2017; Cordero-Morales and Vasquez, 2018; Harayama and Riezman, 2018; Ridone et al., 2018, 2020; Romero et al., 2019). Channel modulation often occurs through the alteration of membrane mechanics. For instance, excluding PUFAs from the diet of *Drosophila melanogaster* increases plasma membrane stiffness and slows light-induced responses mediated by TRP and TRPL channels (Randall et al., 2015). In addition, arachidonic acid modulates NMDA receptor gating by changing the mechanical properties of the lipid bilayer, rather than by binding to specific sites on the receptor (Casado and Ascher, 1998; Kloda et al., 2007). We have previously shown that ω -3 eicosapentaenoic acid (EPA) and its eicosanoid derivative, epoxyeicosatetraenoic acid (17,18-EEQ), enhance TRPV4 activity in cultured human microvascular endothelial cells (HMVECs) through plasma membrane remodeling (Caires et al., 2017). Specifically, ω -3 fatty acids decrease endothelial cell plasma membrane structural order, which favors the TRPV4 open state.

Mammals cannot synthesize precursors of PUFAs. As such, PUFAs must be ingested as components of our diet (Wallis et al., 2002). Diets enriched in ω -3 PUFAs have been associated with several health benefits, including the prevention of vascular dysfunction, inflammation, and thrombosis (Endo and Arita, 2016; Wiest et al., 2016). Recently, it was shown that consuming foods enriched in ω -3 fatty acids improved the prognosis of myocardial infarction (Lazaro et al., 2020). Moreover, ω -3 PUFAs were used as an effective therapy for improving endothelial function and attenuating inflammation associated with metabolic syndromes in humans (Dangardt et al., 2010; Tousoulis et al., 2014). ω -3 PUFA supplementation improves endothelial function and attenuates arterial stiffness in hypertensive patients (Casanova et al., 2017). Likewise, we have shown that EPA decreases the rigidity of HMVEC membranes (Caires et al., 2017). Although there is support for a beneficial effect of ω -3 fatty acids, determining whether a dietary or genetic increase in EPA

can enhance TRPV4-mediated vasodilation would be an important step forward toward the generation of strategies to improve vascular dysfunction.

Here, we combined electrophysiology, myography, lipidomics, and Ca^{2+} imaging experiments to show that dietary or genetic enrichment of EPA increases TRPV4 activation in endothelial cells and TRPV4-mediated vasodilation in an endothelial cell-specific manner. We demonstrate that EPA decreases Ca^{2+} -dependent TRPV4 desensitization to prolong TRPV4-mediated vasodilation. Furthermore, macroscopic current analyses reveal that the TRPV4 proximal N terminus is required for the EPA-mediated reduction in channel desensitization. Our work provides proof of concept that manipulating fatty acid content *in vivo* can modulate the function of a vascular ion channel to enhance vasodilation.

RESULTS

EPA supplementation enhances TRPV4 activity in human primary vascular endothelial cells

There is growing evidence supporting the idea that fatty acids modulate the function of sensory ion channels (Cordero-Morales and Vasquez, 2018; Harayama and Riezman, 2018). Decreasing or increasing channel activity by manipulating the lipid membrane content could be complementary to the use of agonists and antagonists to modulate vascular reactivity. To determine whether EPA increases TRPV4 activity in endothelial cells of a variety of vascular beds, we recorded endogenous TRPV4 currents in primary-cultured human vascular endothelial cells from skin, retina, lung, brain, and aorta, with and without EPA supplementation. EPA significantly increased TRPV4 current activation by GSK1016790A (GSK101), a selective TRPV4 agonist, regardless of the vascular origin of endothelial cells (Figures 1A, 1B, and S1A). EPA supplementation yielded a 5-fold leftward shift in the EC_{50} for GSK101, with values of 237.30 ± 46.02 and 47.80 ± 4.50 nM for control and EPA-treated aortic endothelial cells, respectively (Figure 1C). Next, we asked whether EPA supplementation increases TRPV4 channel expression in endothelial cells, which may explain the larger current density. There was no significant difference in TRPV4 membrane expression levels between control and EPA-treated cells, as determined by western blot analyses (Figures 1D, S1B, and S1C). Parenthetically, the two protein bands observed in the western blot correspond to glycosylated and unglycosylated TRPV4 (relative molecular weights of 139 and 125 kDa, respectively), as reported previously (Xu et al., 2006). Aortic endothelial cells supplemented with EPA had similar resting potentials and membrane capacitance compared with control cells (Figures S1D and S1E), suggesting that EPA does not affect the passive membrane properties of endothelial cells. In addition, EPA supplementation did not alter the function of TRPC3/TRPC6, TRPV1, TRPV3, and TRPA1 channels (Figure S2), known to be expressed in the vasculature (Earley and Brayden, 2015). Taken together, our data show that EPA supplementation increases TRPV4 activity in primary-cultured human vascular endothelial cells from large (conduit) and small (resistance size) vessels.

Mesenteric arteries of *fat-1* mice display enhanced TRPV4-mediated vasodilation

Given the effects of *in vitro* EPA supplementation on TRPV4 currents, we reasoned that channel activity would be higher in endothelial cells of animal models with elevated levels of EPA. The human diet typically contains high levels of ω -6 PUFAs but is deficient in ω -3 fatty acids (Simopoulos, 2016). As mammals cannot convert ω -6 into ω -3 PUFAs (Figure 2A, left panel), the precursors of long ω -3 PUFAs are an essential part of our diet. Unlike mammals, *C. elegans* express the FAT-1 ω -3 desaturase enzyme (Figure 2A, middle panel) (Wallis et al., 2002). The FAT-1 enzyme adds a double bond at the ω -3 position (closest to the terminal methyl group) of 18- or 20-carbon ω -6 PUFAs, generating ω -3 PUFAs (Watts and Browse, 2002). In 2004, Kang and collaborators engineered a transgenic mouse carrying the *fat-1* gene from *C. elegans* (Figure 2A, right panel). The *fat-1* mice display an increased content of ω -3 fatty acids in various organs and tissues, without dietary supplementation (Kang et al., 2004). This mouse model offers the opportunity to measure TRPV4 activity in a genetically enriched ω -3 PUFA environment. Using LC-MS, we found that third- and fourth-order mesenteric arteries of *fat-1* mice had higher EPA-membrane content when compared with those of wild-type (WT) mice (Figure 2B). TRPV4 current densities were larger in primary-cultured mesenteric artery endothelial cells from *fat-1* mice when compared with those from WT (Figures 2C and 2D). These results are comparable with EPA-supplemented primary-cultured human endothelial cells and indicate that TRPV4 activity is increased in an environment where the EPA-membrane content has been genetically increased.

Since TRPV4 is an important regulator of arterial contractility (Earley et al., 2009; Sonkusare et al., 2012), we hypothesized that arteries from *fat-1* mice would exhibit enhanced TRPV4-mediated vasodilation. To this end, we studied pressurized (80 mmHg), myogenic resistance-size mesenteric arteries (third- and fourth-order) from *fat-1* and WT mice. Notably, when challenged with 5 nM GSK101, *fat-1* arteries displayed a 1.6-fold larger vasodilation than WT arteries (Figures 3A and 3B). In contrast, diameter at low pressure (10 mmHg), myogenic tone, depolarization-induced vasoconstriction, and passive diameter at 80 mmHg were all similar in arteries of *fat-1* and WT mice (Figures S3A–S3D). These results indicate that *fat-1* expression does not alter the contractile function of arteries. Endothelium denudation abolished GSK101-induced vasodilation in mesenteric arteries from WT and *fat-1* mice (Figure 3B). This result indicates that EPA enrichment enhances TRPV4-dependent vasodilation in an endothelium-dependent manner. Next, we measured TRPV4 membrane expression in arteries from *fat-1* and WT mice. No differences were observed in TRPV4 membrane expression between WT and *fat-1* mesenteric arteries, in agreement with our data from primary-cultured human endothelial cells (Figures 3C, 3D, and S3E). Our findings demonstrate that a genetically induced elevation in EPA-membrane content increases TRPV4-mediated vasodilation in an endothelium-dependent manner.

An ω -3 fatty acid-enriched diet enhances TRPV4-mediated vasodilation

Diets enriched in ω -3 fatty acids, such as fish oil and flaxseed, have been linked with a wide range of health benefits, including cardiovascular function (Swanson et al., 2012). However, the molecular targets of ω -3 fatty acids and the signaling processes they modulate are unclear. Our results with the *fat-1* mouse model support that increased EPA-membrane

content has the potential to increase TRPV4-mediated vasodilation. Next, we tested the hypothesis that an EPA-enriched diet can also increase TRPV4-mediated vasodilation. Menhaden oil is a natural source of ω -3 fatty acids that contains ~13% EPA (Ossani et al., 2015). Accordingly, we fed C57BL/6J mice a diet enriched in menhaden oil for 8 weeks. The body weight of animals fed standard or ω -3 fatty acid-enriched diets was similar (Figure S4A). EPA-membrane content was higher in resistance-size mesenteric arteries from mice fed an ω -3 fatty acid-enriched diet when compared with that of mice fed a standard diet, as determined by LC-MS (Figure 4A). GSK101 stimulated larger vasodilation in pressurized mesenteric arteries of mice fed an ω -3 fatty acid-enriched diet than those given a standard diet (Figures 4B and 4C). Furthermore, GSK101-induced vasodilation in arteries of mice fed an ω -3 fatty acid-enriched diet maintained a plateau that was not observed in arteries of standard diet mice (Figure 4B). Vasodilation at the end of the GSK101 stimuli was 4-fold larger in arteries from mice fed an ω -3 fatty acid-enriched diet than those fed the standard diet (Figure 4D). The arterial diameter at low pressure, myogenic tone, depolarization-induced vasoconstriction, and passive diameter were all similar in arteries of mice fed either an ω -3 fatty acid-enriched or standard diet (Figures S4B–S4E).

As observed in primary-cultured human endothelial cells and *fat-1* mice mesenteric arteries, TRPV4 membrane expression was similar in the arteries of WT mice fed an ω -3 fatty acid-enriched or standard diet (Figures 4E and S4F). GSK101 evoked a larger increase in TRPV4 current density in endothelial cells from mice fed an ω -3 fatty acid-enriched diet when compared with the standard (Figures 4F and 4G). To determine the contribution of smooth muscle cells to these responses, we induced vasodilation with sodium nitroprusside (SNP), a nitric oxide donor. SNP-mediated vasodilation was similar in arteries from mice fed either an ω -3 fatty acid-enriched or standard diet (Figure 4H). In summary, these data demonstrate that an ω -3 fatty acid-enriched diet increases TRPV4-mediated vasodilation in an endothelial cell-specific manner.

An ω -3 fatty acid-enriched diet slows TRPV4-mediated vasodilation decay in *fat-1* mice

GSK101-induced vasodilation decay of *fat-1* mouse arteries was more pronounced (Figure 3A) than in arteries from WT mice fed an ω -3 fatty acid-enriched diet (Figure 4B). EPA-membrane content was higher in mesenteric arteries from animals fed an ω -3 fatty acid-enriched diet (Figure 4A) than in arteries from *fat-1* mice (Figure 2B), suggesting that dietary supplementation is more efficient at accumulating this PUFA. These results support the concept that EPA-membrane content in mice fed an ω -3 fatty acid-enriched diet could further attenuate the decay that occurs during TRPV4-mediated vasodilation. To test this hypothesis, we fed *fat-1* mice an ω -3 fatty acid-enriched diet, which increased EPA-membrane content in their mesenteric arteries more than in those from *fat-1* mice on a standard diet (Figure 5A). The magnitude of GSK101-induced dilation was similar in arteries from *fat-1* mice fed a standard or ω -3 fatty acid-enriched diet (Figures 5B and 5C). As expected, *fat-1* mice fed an ω -3 fatty acid-enriched diet displayed a slower GSK101-induced dilation decay than *fat-1* mice fed a standard diet (Figure 5D). The body weight of *fat-1* mice fed either standard or ω -3 fatty acid-enriched diets was similar (Figure S5A). These results support that additional accumulation of EPA membrane content slows the decay of TRPV4-mediated vasodilation.

EPA decreases TRPV4 Ca²⁺-dependent desensitization

TRPV4 undergoes a desensitization process in the presence of Ca²⁺ (Caires et al., 2017; Jin et al., 2011; Watanabe et al., 2002b). We hypothesized that EPA enhances and prolongs maximal TRPV4-induced vasodilation by decreasing TRPV4 Ca²⁺-dependent endothelial desensitization. To this end, we characterized TRPV4 desensitization with or without EPA supplementation. EPA treatment yielded larger GSK101-elicited currents and reduced TRPV4 Ca²⁺-dependent desensitization in human aortic endothelial cells (Figures 6A–6C). Next, we measured fluorescence intensity changes (indicative of changes in intracellular Ca²⁺) as a readout of TRPV4 activity in isolated and cultured endothelial cells from third- and fourth-order mesenteric arteries, loaded with a Ca²⁺-sensitive dye (Fluo-4 AM), from mice fed an ω -3 fatty acid-enriched or standard diet. We observed a marked difference in the GSK101 response profile, such that cells isolated from mice fed an ω -3 fatty acid-enriched diet displayed larger and prolonged increases in intracellular Ca²⁺ compared with cells from mice fed a standard diet (Figures 6D and 6E). This is further apparent when comparing the area under the fluorescence intensity curves elicited by GSK101 (Figure 6F).

TRPV4 has been shown to be activated downstream of osmolarity changes and shear stress, enabling endothelial cells to transduce hemodynamic forces (Hartmannsgruber et al., 2007; Liedtke et al., 2000; Strotmann et al., 2000; White et al., 2016; Wissenbach et al., 2000). Therefore, we tested the response of isolated and cultured endothelial cells, from animals fed an ω -3 fatty acid-enriched or standard diet, to osmotic changes. A hypoosmotic challenge evoked larger and prolonged increases in intracellular Ca²⁺ in cells from mice fed an ω -3 fatty acid-enriched diet compared with those fed a standard diet (Figures 6G–6I). These results are similar to those obtained with GSK101. Taken together, EPA reduces TRPV4 Ca²⁺-dependent desensitization and attenuates the decay in vasodilation that occurs in mesenteric arteries.

The TRPV4 N terminus mediates the effect of EPA on channel desensitization

Lipid membranes highly enriched in ω -3 PUFAs have distinct mechanical properties, such as increased disorder and low bending stiffness (Caires et al., 2017; Mason et al., 2016; Romero et al., 2019). Changes in the mechanical properties of the plasma membrane could modulate channel function through specific protein domains. Several reports have shown that the TRPV4 N terminus interacts with the plasma membrane, via PIP₂ or PACSIN3 (a BAR-domain-containing protein), to modulate channel function (D'Hoedt et al., 2008; Garcia-Elias et al., 2013). Based on these studies, we hypothesized that the TRPV4 N terminus might play a role in the modulation of channel function by EPA-enriched membranes. To test this hypothesis, we engineered a *Trpv4* construct lacking the first 186 amino acid residues (Figures 7A, 7D, and S5B) and determined its Ca²⁺-dependent desensitization with or without EPA supplementation. Macroscopic current analyses indicated that EPA does not alter 186 rat TRPV4 Ca²⁺-dependent desensitization, in contrast to what is observed with the full-length *Trpv4* construct (Figures 7A–7F). Importantly, neutralizing a cluster of positive charges at the N terminus (Lys121, Arg122, Arg124, Arg125, Lys126), previously recognized as a TRPV4-PIP₂ interaction site (Garcia-Elias et al., 2013), abolished the effect of EPA on TRPV4 Ca²⁺-dependent desensitization (Figures 7G–7I). The functional difference between these constructs is also underscored

when comparing the time required to decay to half of the maximal current (Figures 7C, 7E, and 7I). Our findings support that the TRPV4 proximal N terminus mediates the effect of EPA on channel desensitization.

DISCUSSION

TRPV4 activation promotes vasodilation by increasing intracellular Ca^{2+} , followed by the activation of Ca^{2+} -activated potassium channels, nitric oxide release, and subsequent smooth muscle cell hyperpolarization (Earley et al., 2005, 2009; Kohler et al., 2006; Sonkusare et al., 2012). Several lines of evidence suggest that reduced TRPV4 expression and function underlie endothelial impairment associated with cardiovascular disease risk factors, including hypertension, obesity, diabetes, and aging (Goto and Kitazono, 2021). For example, TRPV4 expression and function are markedly reduced in the endothelial cells of various vascular beds in rat models of aging and diabetes, as well as in mouse models of obesity-induced hypertension, where vasodilation is compromised (Du et al., 2016; Ottolini et al., 2020; Shamsaldeen et al., 2020). Hence, it is apparent that treatments that increase TRPV4 expression and/or activity could ameliorate endothelial dysfunction and alleviate cardiovascular diseases.

Dietary consumption of ω -3 PUFAs, which are present in fish oils, is known to prevent vascular dysfunction (Wiest et al., 2016). However, the molecular targets of ω -3 PUFAs remain unclear. Previously, we proposed a model in which ω -3 fatty acid metabolism provides a membrane environment favorable for TRPV4 activity, while channels outside these plasma membrane domains display less activity (Caires et al., 2017). Consequently, our overarching question is whether a fatty acid dietary intervention could be used to improve vascular reactivity. We have addressed this question and demonstrated that genetic- and diet-induced ω -3 fatty acid enrichment reduces TRPV4 desensitization in endothelial cells and enhances arterial vasodilation. In this work, we investigated the effect of ω -3 fatty acid enrichment on TRPV4-mediated vasodilation of pressurized third- and fourth-order mesenteric arteries. Several lines of evidence demonstrate that ω -3 fatty acid enrichment enhances TRPV4-mediated vasodilation. First, a mouse model carrying the *fat-1* gene, which encodes FAT-1, a *C. elegans* ω -3 desaturase enzyme that converts ω -6 into ω -3 PUFAs, exhibits higher EPA-membrane content in mesenteric arteries, increased TRPV4 channel activity, and enhanced TRPV4-mediated vasodilation. Second, feeding WT animals a menhaden oil-enriched diet increases EPA-membrane content in mesenteric arteries and increases TRPV4 function, as well as eliciting larger and maintained TRPV4-mediated vasodilation in an endothelial cell-specific manner. Third, elevating EPA-membrane content decreases TRPV4 Ca^{2+} -dependent endothelial desensitization in response to chemical and physical stimuli.

How do EPA-enriched membranes enhance channel function and TRPV4-mediated vasodilation? TRPV4 is activated by various physiological stimuli, including mild temperatures and chemical ligands, as well as downstream of osmolarity changes and shear stress (Hartmannsgruber et al., 2007; Liedtke et al., 2000; Strotmann et al., 2000; Thorneloe et al., 2008; Vriens et al., 2004; Watanabe et al., 2002a, 2002b; Wissenbach et al., 2000). We have previously shown that membranes enriched in EPA enhance TRPV4 function

regardless of the nature of the stimuli (e.g., chemical or physical) (Caires et al., 2017). For instance, we showed that EPA enhances rat TRPV4 activation by GSK101, Phorbol (4 α -PDD), osmolarity, and downstream of mechanical stimulation in *C. elegans*. Here, we also show that endothelial cells isolated from mesenteric arteries of mice fed with an EPA-enriched diet display larger and more prolonged fluorescence responses (indicative of an increase in intracellular Ca²⁺), when compared with mice fed with a standard diet, after a chemical or hypoosmotic challenge. Hence, we envision that a diet enriched in EPA could favor TRPV4-mediated vasodilation when faced with endogenous agonists or changes in osmolarity and shear stress *in vivo*.

Lipid headgroups and acyl chains are major determinants of membrane physicochemical properties (e.g., organization, spontaneous curvature, bending stiffness) (Harayama and Riezman, 2018; Lorent et al., 2020). For instance, plasma membranes enriched in saturated fatty acids are ordered, tightly packed, and rigid, whereas high levels of polyunsaturation yield relatively fluid and loosely packed membranes (Lorent et al., 2020). We have demonstrated that plasma membranes highly enriched in EPA are less organized, more fluid, and display a low bending stiffness (Caires et al., 2017; Romero et al., 2019). The conclusion emerging from our work is that these loosely packed membranes favor TRPV4 channel opening (requiring less agonist) and oppose time-dependent desensitization. We propose that modifying the mechanical properties of the plasma membrane slows TRPV4 channel desensitization in endothelial cells and attenuates the decay in vasodilation. EPA-enriched membranes could also recruit or exclude lipids, or proteins with lipid-binding domains that regulate TRPV4 activity. Several classes of proteins interact with the membrane by sensing its mechanical properties, including BAR-domain-containing proteins, which are known to sense membrane curvature (Harayama and Riezman, 2018). There is evidence that PACSIN3, a cytoplasmic protein member of the F-BAR domain family, binds to TRPV4 and negatively affects channel function (Cuajungco et al., 2006; D'Hoedt et al., 2008; Garcia-Elias et al., 2013; Goretzki et al., 2018). In the context of our results, it is possible that EPA enrichment decreases this TRPV4-PACSIN3 inhibitory interaction. Furthermore, there is evidence suggesting that a TRPV4 N terminus interaction with PIP₂ enhances channel activation (Garcia-Elias et al., 2013; Goretzki et al., 2018). Our results with the 186- and the 5Ala-TRPV4 constructs support the idea that EPA enrichment could increase TRPV4 channel function by facilitating the interaction between the proximal N terminus and membrane phospholipids. On the other hand, previous work supports that PIP₂ depletion promotes TRPV4 channel activity (Harraz et al., 2018; Takahashi et al., 2014). Future research should determine whether EPA positively or negatively modifies interactions between TRPV4 and various lipid classes.

What is the potential use of modulating TRPV4 function with fatty acids? Previous work has shown that intravenous administration of GSK101 induced a dose-dependent reduction in blood pressure, followed by a profound circulatory collapse in mice, rats, and dogs, whereas no acute cardiovascular effects were observed in TRPV4^{-/-} null mice (Pankey et al., 2014; Willette et al., 2008). The circulatory collapse after activation has hindered efforts to target TRPV4 as antihypertensive therapy. We envision that increasing TRPV4-mediated vasodilation using ω -3 fatty acid-enriched diets could have a more subtle effect on reducing blood pressure, while attenuating arterial stiffness and improving vascular function. On the

other hand, it has been shown that TRPV4 inhibitors counteract edema and inflammation, as well as improve pulmonary function (Balakrishna et al., 2014). We speculate that a combination of a higher ω -6: ω -3 fatty acid diet ratio, achieved by increasing dietary ω -6 PUFAs, together with TRPV4 inhibitors, might be beneficial in treating conditions in which reduced TRPV4 activity is desired.

The data presented here provide a basis for understanding the beneficial effects of ω -3 fatty acids in the vasculature. Our work provides proof of concept that increasing ω -3 fatty acid content *in vivo* can regulate TRPV4 function. Establishing the chemical and structural bases whereby EPA endows membranes with distinct properties favoring the TRPV4 open state could help identify molecules that mimic its effect, serving as potential therapies to improve vascular reactivity. Beyond the role of TRPV4 in the vasculature, our approach of manipulating the membrane lipid content *in vivo* could be extended to modulate ion channels in other organ systems.

Limitations of the study

In this work, we focused on determining the effect of EPA membrane enrichment on TRPV4-mediated vasodilation. Although we found that EPA does not enhance the function of other TRP channels expressed in mesenteric endothelial cells, the effect of this fatty acid on other membrane proteins or vasodilators, independent of TRPV4, was not evaluated in this study. EPA membrane enrichment enhances TRPV4 channel function in endothelial cells from large (conduit) and small (resistance size) vessels. Hence, we expect that EPA treatment would enhance TRPV4-mediated vasodilation regardless of the vascular bed. However, we did not determine the effect of TRPV4-mediated vasodilation in other arteries.

STAR★METHODS

RESOURCE AVAILABILITY

Lead contact—Further information and requests for resources and reagents should be directed to and will be fulfilled by the lead contact, Julio F. Cordero-Morales (jcordero@uthsc.edu).

Materials availability—The plasmids generated in this study are available from the lead contact (Julio F. Cordero-Morales; jcordero@uthsc.edu).

Data and code availability

- The source data underlying figures and supplementary figures are provided as a source data file and deposited at figshare [10.6084/m9.figshare.16692073](https://www.figshare.com/figure/10.6084/m9.figshare.16692073). Original western blot images are available in the supplemental information.
- This paper does not report original code.
- Any additional information required to reanalyze the data reported in this paper is available from the lead contact upon request.

EXPERIMENTAL MODELS AND SUBJECT DETAILS

Cell lines

Primary human endothelial cells: Primary-cultured human vascular endothelial cells from skin, retina, lung, brain, and aorta were obtained at passage 4 from Cell Systems (<https://cell-systems.com>). Cells were cultured according to the manufacturer's protocol and used until the 7th passage.

HEK 293 cells: Human embryonic kidney cells (HEK 293) obtained from the American Type Culture Collection (ATCC®) were cultured in DMEM, supplemented with 10% fetal bovine serum and 1% penicillin-streptomycin at 37°C and 5% CO₂.

Animals: All procedures performed in this work were reviewed and approved by the University of Tennessee Health Science Center Institutional Animal Care and Use Committee (IACUC). All methods were carried out in accordance with the approved guidelines. C57BL/6J and C57BL/6-Tg (CAG-*fat-1*)1Jxk/J mice were initially purchased from Jackson Laboratories and bred to maintain the *fat-1* transgene in heterozygosis. Male mice were fed for 6–8 weeks with an enriched-fatty acid diet or standard diet, starting at 8 weeks of age. Food and water were provided *ad libitum* and mice were kept with 12 h:12 h light/dark cycles. Enriched-fatty acid diets were purchased from Dyets Inc. For all experiments, mice were euthanized with isoflurane (1.5%), followed by decapitation.

METHOD DETAILS

Cell culture and patch-clamp electrophysiology—Endothelial cells were incubated overnight with 100 μ M EPA (C20:5; Nu-Chek Prep, Inc.) enriched media before electrophysiological measurements. We perfused 0.1–2 μ M GSK1016790A (GSK101; Tocris) to activate TRPV4 channels. These currents were inhibited by 5 μ M HC067047 (HC; Sigma-Aldrich). Recording electrode pipettes were made of borosilicate glass (O.D.: 1.5 mm from Sutter Instruments) and fire-polished to obtain a resistance between 4–5.5 M Ω . Macroscopic currents were recorded with an Axopatch 200A amplifier (Molecular Devices, Union City, CA, USA), using 1 s voltage ramps from –80 to +80 mV from a holding potential of –60 mV, and a Digidata 1555A digitizer (Molecular Devices) with a sample rate of 10 KHz. Data was analyzed off-line using Clampfit v10.4 (Molecular Devices). For whole-cell recordings the bath solution contained (in mM): 140 NaCl, 6 KCl, 1 MgCl₂, 10 Glucose and 10 HEPES (pH 7.3) and the pipette solution contained (in mM): 140 CsCl, 5 EGTA and 10 HEPES (pH 7.2). For desensitization experiments, endothelial cells (Cell Systems) and HEK 293 cells were recorded at a constant voltage of –60 mV in the whole-cell configuration using a bath solution containing (in mM): 140 NaCl, 6 KCl, 1 MgCl₂, 5 CaCl₂, 10 Glucose, and 10 HEPES (pH 7.4) and a pipette solution containing (in mM): 140 CsCl, and 10 HEPES (pH 7.2). HEK293 cells were co-transfected with 50 ng*mL⁻¹ GFP-pMO (a pcDNA3.1-based vector with the 5' and -3' untranslated regions of the beta-globin gene) and either 80 ng*mL⁻¹ full-length rat *Trpv4* or 1.5 μ g*mL⁻¹ 186 rat *Trpv4*-pMO or 5A1a (K121A, R122A, R124A, R125A, K126A) rat *Trpv4* using Lipofectamine 2000 (Thermo Fisher Scientific), according to the manufacturer's instructions.

Primary-cultured endothelial cells were obtained from mesenteric artery branches collected and placed into ice-cold physiological saline solution (PSS) that contained (in mM): 112 NaCl, 6 KCl, 24 NaHCO₃, 1.8 CaCl₂, 1.2 MgSO₄, 1.2 KH₂PO₄, and 10 glucose, then gassed with 21% O₂, 5% CO₂, and 74% N₂ (pH 7.4), and cleaned of adventitial tissue. Immediately after collection, the artery was cannulated, perfused intraluminally, and incubated with endothelial cell growth medium (serum-free, PromoCell) containing 2 mg/mL of collagenase type 2 (Worthington) for 30–40 min at 37°C. Endothelial cells were flushed out from the artery using the endothelial cell growth medium (serum-free). Isolated cells were placed into the endothelial cell growth medium (containing serum) and seeded onto glass coverslips pre-treated with gelatin in a 35 mm diameter petri dish. The growth medium was changed after 24 h and every 2 days until electrophysiological recordings were performed (5–7 days later). For whole-cell recordings the bath solution contained (in mM): 140 NaCl, 6 KCl, 2 CaCl₂, 1 MgCl₂, 10 Glucose and 10 HEPES (pH 7.3) and the pipette solution contained (in mM): 140 CsCl, 5 EGTA and 10 HEPES (pH 7.2).

Diet supplementation—A) Standard diet (sd; #7012 ENVIGO; UTHSC animal facility diet; (<https://insights.envigo.com/hubfs/resources/data-sheets/7012-datasheet-0915.pdf>)); B) Menhaden oil-supplemented (enriched in EPA, Dyets Inc. # 112246). Modified AIN-93G Purified Rodent Diet with 59% Fat Derived Calories from Menhaden Oil (kcal/kg): Casein (716), L-Cystine (12), Maltose Dextrin (502), Cornstarch (818.76), Menhaden oil (2430), Soybean Oil (630), Mineral Mix (# 210025; 30.8), and Vitamin Mix (#310025; 38.7).

Pressurized arterial myography—Experiments were performed with isolated mouse 3rd and 4th order mesenteric arteries. Dissected arteries were placed in PSS (described above). Arterial segments of 1–2 mm in length were cannulated at each end in a chamber (Living Systems Instrumentation) that was continuously perfused with PSS. We perfused 5 nM GSK1016790A (GSK101) to elicit TRPV4-mediated vasodilation and 60 mM KCl to elicit vasoconstriction. Solutions and the chamber were maintained at 37°C. Intravascular pressure was altered using an attached reservoir and monitored using a pressure transducer. Luminal flow was absent during experiments. The arterial diameter was measured at 1 Hz using a CCD camera attached to a Nikon TS100-F microscope and the automatic edge-detection function of IonWizard software (Ionoptix). The myogenic tone was calculated as $100 \times (1 - D_{\text{active}}/D_{\text{passive}})$, where D_{active} is active arterial diameter, and D_{passive} is the diameter determined in the presence of Ca²⁺-free PSS (supplemented with 5 mM EGTA). The percentage change in diameter in response to either 5 nM GSK101 or 60 mM K⁺ was calculated as:

$$\frac{\text{diameter change} - \text{control diameter}}{\text{control diameter}} \times 100$$

Protein expression determination—Primary-cultured human endothelial cells were collected as previously described (Caires et al., 2017). Whole arteries were cut into small pieces and dissociated mechanically with a pellet pestle motor (Kimble) in a cold Cell Wash Solution (with Halt Protease Inhibitor Cocktail and 1X EDTA, ThermoFisher Scientific). Cells or arteries were treated with the Mem-PER Plus Membrane Protein Extraction Kit

(ThermoFisher Scientific). Cells or arteries were washed twice with cold Cell Wash Solution (with Halt Protease Inhibitor Cocktail and 1X EDTA). Pelleted cells were resuspended with cold Permeabilization Buffer (with Halt Protease Inhibitor Cocktail and 1X EDTA) and homogenized with a sonicator. The solution was then incubated for 10 min with constant mixing at 4°C. Homogenates were spun down at 16,000 *g* for 15 min at 4°C. Permeabilized cells were resuspended in cold Membrane Solubilization Buffer (with Halt Protease Inhibitor Cocktail and 1X EDTA) and incubated for 30 min at 4°C with constant mixing. Solubilized cells were spun down at 16,000 *g* for 15 min at 4°C. Supernatants containing solubilized membrane proteins were transferred to a new tube. The collected supernatants were subjected to acetone precipitation, whereby cold acetone (−20°C) was added at a volume 4 times that of the sample volume, briefly vortexed, and incubated at −20°C for 60 min. Samples were centrifuged at 15,000 *g* for 10 min at 4°C. Acetone was removed, then precipitated protein pellets were air-dried and dissolved in 1X PBS. Protein concentration was measured with the Bio-Rad protein assay and $\cong 10 \mu\text{g}$ of total protein was loaded in Mini-PROTEAN TGX Stain-Free Precast Gels (Bio-Rad). Rabbit polyclonal anti-human TRPV4 (1:300; Abcepta # AP18990a) and goat anti-rabbit IgG HL-HRP conjugated (1:3,000; Bio-Rad #1706515) antibodies were used for western blots. Membranes were developed with Clarity Max Western ECL Substrate (Bio-Rad) and imaged in a ChemiDoc Touch Imaging System (Bio-Rad) for chemiluminescence. Western blots were analyzed using Image Lab Software (Bio-Rad) to normalize chemiluminescent signals against total protein measured from the stain-free signal in the corresponding lane.

Liquid chromatography-mass spectrometry—Whole arteries were collected and cleaned as previously described, washed in PSS buffer, and frozen in liquid N₂. Primary human vascular endothelial cells were cultured according to the manufacturer's protocol, up to 2–4 million cells per sample. Cells were rinsed with PBS three times and frozen in liquid nitrogen. Total and free fatty acids were extracted and quantified at the Lipidomics Core Facility at Wayne State University. Membrane (i.e., esterified) fatty acids were determined by subtracting free from total fatty acids and normalized by the number of cells in the culture or total protein.

Calcium imaging—Mesenteric endothelial cells were cultured, as previously described above, and loaded with 1 μM Fluo4-AM (ThermoFisher Scientific), according to the manufacturer's protocol. Micrographs were acquired in an upright Olympus BX51WI microscope with a 10X water immersion objective (numerical aperture 0.3) and analyzed using CellSens software (Olympus). The bath solution contained (in mM): 105 NaCl, 5 CaCl₂, 1 MgCl₂, 10 HEPES, 10 Glucose and 90 Mannitol (320 mOsm; pH 7.3), with or without 0.1–1 μM GSK101. For the hypotonic stimuli, the solution contained (in mM): 105 NaCl, 5 CaCl₂, 1 MgCl₂, 10 HEPES, and 10 glucose (240 mOsm) (pH 7.3). Data analysis was performed offline using OriginLab.

QUANTIFICATION AND STATISTICAL ANALYSES

OriginLab was used for plotting. Statistical analyses were performed using GraphPad InStat 3 software, OriginLab, and Estimation Stats (Ho et al., 2019). Individual statistical tests,

number of samples, dispersion and precision measures, and significance are described in each figure legend. Statistical significance was established at 95% confidence.

Sigmoidal fitting was done using OriginPro with the following Hill equation:

$$f(x) = V_{max} \frac{x^n}{k^n + x^n}$$

where V_{max} is max velocity, k is the Michaelis constant, and n cooperative sites.

Supplementary Material

Refer to Web version on PubMed Central for supplementary material.

ACKNOWLEDGMENTS

The authors thank graduate student Briar Bell for critically reading the manuscript and members of the Vásquez and Cordero-Morales groups for technical support. We thank Dr. Somdatta Saha for technical support with western blot analyses. We used the Lipidomics Core Facility at Wayne State University for lipid analyses. The core facility is supported in part by the National Center for Research Resources, National Institutes of Health Grant (S10RR027926). This work was supported by the National Institutes of Health (R01GM133845 to V.V.; R01HL133256, R01HL155180, and R01HL158846 to J.H.J.; and R01GM125629 to J.F.C.-M.) and the Neuroscience Institute at UTHSC (Postdoctoral Matching Salary Support to R.C.).

REFERENCES

- Alvarez DF, King JA, Weber D, Addison E, Liedtke W, and Townsley MI (2006). Transient receptor potential vanilloid 4-mediated disruption of the alveolar septal barrier: a novel mechanism of acute lung injury. *Circ. Res* 99, 988–995. 10.1161/01.RES.0000247065.11756.19. [PubMed: 17008604]
- Balakrishna S, Song W, Achanta S, Doran SF, Liu B, Kaelberer MM, Yu Z, Sui A, Cheung M, Leishman E, et al. (2014). TRPV4 inhibition counteracts edema and inflammation and improves pulmonary function and oxygen saturation in chemically induced acute lung injury. *Am. J. Physiol. Lung Cell Mol. Physiol* 307, L158–L172. 10.1152/ajplung.00065.2014. [PubMed: 24838754]
- Baylie RL, and Brayden JE (2011). TRPV channels and vascular function. *Acta Physiol.* 203, 99–116. 10.1111/j.1748-1716.2010.02217.x.
- Caires R, Sierra-Valdez FJ, Millet JRM, Herwig JD, Roan E, Vásquez V, and Cordero-Morales JF (2017). Omega-3 fatty acids modulate TRPV4 function through plasma membrane remodeling. *Cell Rep.* 21, 246–258. 10.1016/j.celrep.2017.09.029. [PubMed: 28978477]
- Casado M, and Ascher P (1998). Opposite modulation of NMDA receptors by lysophospholipids and arachidonic acid: common features with mechanosensitivity. *J. Physiol* 513, 317–330. 10.1111/j.1469-7793.1998.317bb.x. [PubMed: 9806985]
- Casanova MA, Medeiros F, Trindade M, Cohen C, Oigman W, and Neves MF (2017). Omega-3 fatty acids supplementation improves endothelial function and arterial stiffness in hypertensive patients with hypertriglyceridemia and high cardiovascular risk. *J. Am. Soc. Hypertens* 11, 10–19. 10.1016/j.jash.2016.10.004. [PubMed: 27876342]
- Cordero-Morales JF, and Vásquez V (2018). How lipids contribute to ion channel function, a fat perspective on direct and indirect interactions. *Curr. Opin. Struct. Biol* 51, 92–98. 10.1016/j.sbi.2018.03.015. [PubMed: 29602157]
- Cuajungco MP, Grimm C, Oshima K, D’Hoedt D, Nilius B, Mensenkamp AR, Bindels RJM, Plomann M, and Heller S (2006). PACSINs bind to the TRPV4 cation channel. PACSIN 3 modulates the subcellular localization of TRPV4. *J. Biol. Chem* 281, 18753–18762. 10.1074/jbc.M602452200. [PubMed: 16627472]

- Dangardt F, Osika W, Chen Y, Nilsson U, Gan LM, Gronowitz E, Strandvik B, and Friberg P (2010). Omega-3 fatty acid supplementation improves vascular function and reduces inflammation in obese adolescents. *Atherosclerosis* 212, 580–585. 10.1016/j.atherosclerosis.2010.06.046. [PubMed: 20727522]
- D’Hoedt D, Owsianik G, Prenen J, Cuajungco MP, Grimm C, Heller S, Voets T, and Nilius B (2008). Stimulus-specific modulation of the cation channel TRPV4 by PACSIN 3. *J. Biol. Chem* 283, 6272–6280. 10.1074/jbc.M706386200. [PubMed: 18174177]
- Du J, Wang X, Li J, Guo J, Liu L, Yan D, Yang Y, Li Z, Zhu J, and Shen B (2016). Increasing TRPV4 expression restores flow-induced dilation impaired in mesenteric arteries with aging. *Sci. Rep* 6, 22780. 10.1038/srep22780. [PubMed: 26947561]
- Earley S, and Brayden JE (2015). Transient receptor potential channels in the vasculature. *Physiol. Rev* 95, 645–690. 10.1152/physrev.00026.2014. [PubMed: 25834234]
- Earley S, Heppner TJ, Nelson MT, and Brayden JE (2005). TRPV4 forms a novel Ca²⁺ signaling complex with ryanodine receptors and BKCa channels. *Circ. Res* 97, 1270–1279. 10.1161/01.RES.0000194321.60300.d6. [PubMed: 16269659]
- Earley S, Pauyo T, Drapp R, Tavares MJ, Liedtke W, and Brayden JE (2009). TRPV4-dependent dilation of peripheral resistance arteries influences arterial pressure. *Am. J. Physiol. Heart Circ. Physiol* 297, H1096–H1102. 10.1152/ajpheart.00241.2009. [PubMed: 19617407]
- Endo J, and Arita M (2016). Cardioprotective mechanism of omega-3 polyunsaturated fatty acids. *J. Cardiol* 67, 22–27. 10.1016/j.jjcc.2015.08.002. [PubMed: 26359712]
- Filosa JA, Yao X, and Rath G (2013). TRPV4 and the regulation of vascular tone. *J. Cardiovasc. Pharmacol* 61, 113–119. 10.1097/FJC.0b013e318279ba42. [PubMed: 23107877]
- Garcia-Elias A, Mrkonjic S, Pardo-Pastor C, Inada H, Hellmich UA, Rubio-Moscardó F, Plata C, Gaudet R, Vicente R, and Valverde MA (2013). Phosphatidylinositol-4, 5-bisphosphate-dependent rearrangement of TRPV4 cytosolic tails enables channel activation by physiological stimuli. *Proc. Natl. Acad. Sci. USA* 110, 9553–9558. 10.1073/pnas.1220231110. [PubMed: 23690576]
- Goretzki B, Glogowski NA, Diehl E, Duchardt-Ferner E, Hacker C, Gaudet R, and Hellmich UA (2018). Structural basis of TRPV4 N terminus interaction with syndapin/PACSIN1-3 and PIP2. *Structure* 26, 1583–1593.e5. 10.1016/j.str.2018.08.002. [PubMed: 30244966]
- Goto K, and Kitazono T (2021). The transient receptor potential vanilloid 4 channel and cardiovascular disease risk factors. *Front. Physiol* 12, 728979. 10.3389/fphys.2021.728979. [PubMed: 34616307]
- Grace MS, Bonvini SJ, Belvisi MG, and McIntyre P (2017). Modulation of the TRPV4 ion channel as a therapeutic target for disease. *Pharmacol. Ther* 177, 9–22. 10.1016/j.pharmthera.2017.02.019. [PubMed: 28202366]
- Harayama T, and Riezman H (2018). Understanding the diversity of membrane lipid composition. *Nat. Rev. Mol. Cell Biol* 19, 281–296. 10.1038/nrm.2017.138. [PubMed: 29410529]
- Harraz OF, Longden TA, Hill-Eubanks D, and Nelson MT (2018). PIP2 depletion promotes TRPV4 channel activity in mouse brain capillary endothelial cells. *Elife* 7, e38689. 10.7554/eLife.38689. [PubMed: 30084828]
- Hartmannsgruber V, Heyken WT, Kacik M, Kaistha A, Grgic I, Harteneck C, Liedtke W, Hoyer J, and Köhler R (2007). Arterial response to shear stress critically depends on endothelial TRPV4 expression. *PLoS One* 2, e827. 10.1371/journal.pone.0000827. [PubMed: 17786199]
- Ho J, Tumkaya T, Aryal S, Choi H, and Claridge-Chang A (2019). Moving beyond P values: data analysis with estimation graphics. *Nat. Methods* 16, 565–566. 10.1038/s41592-019-0470-3. [PubMed: 31217592]
- Jin M, Wu Z, Chen L, Jaimes J, Collins D, Walters ET, and O’Neil RG (2011). Determinants of TRPV4 activity following selective activation by small molecule agonist GSK1016790A. *PLoS One* 6, e16713. 10.1371/journal.pone.0016713. [PubMed: 21339821]
- Kang JX, Wang J, Wu L, and Kang ZB (2004). Transgenic mice: fat-1 mice convert n-6 to n-3 fatty acids. *Nature* 427, 504. 10.1038/427504a. [PubMed: 14765186]
- Kloda A, Lua L, Hall R, Adams DJ, and Martinac B (2007). Liposome reconstitution and modulation of recombinant N-methyl-D-aspartate receptor channels by membrane stretch. *Proc. Natl. Acad. Sci. USA* 104, 1540–1545. 10.1073/pnas.0609649104. [PubMed: 17242368]

- Köhler R, Heyken WT, Heinau P, Schubert R, Si H, Kacik M, Busch C, Grgic I, Maier T, and Hoyer J (2006). Evidence for a functional role of endothelial transient receptor potential V4 in shear stress-induced vasodilatation. *Arterioscler. Thromb. Vasc. Biol* 26, 1495–1502. 10.1161/01.ATV.0000225698.36212.6a. [PubMed: 16675722]
- Lázaro I, Rueda F, Cediel G, Ortega E, García-García C, Sala-Vila A, and Bayés-Genís A (2020). Circulating omega-3 fatty acids and incident adverse events in patients with acute myocardial infarction. *J. Am. Coll. Cardiol* 76, 2089–2097. 10.1016/j.jacc.2020.08.073. [PubMed: 33121716]
- Liedtke W, Choe Y, Martí-Renom MA, Bell AM, Denis CS, Sali A, Hudspeth AJ, Friedman JM, and Heller S (2000). Vanilloid receptor-related osmotically activated channel (VR-OAC), a candidate vertebrate osmoreceptor. *Cell* 103, 525–535. [PubMed: 11081638]
- Lorent JH, Levental KR, Ganesan L, Rivera-Longsworth G, Sezgin E, Doktorova M, Lyman E, and Levental I (2020). Plasma membranes are asymmetric in lipid unsaturation, packing and protein shape. *Nat. Chem. Biol* 16, 644–652. 10.1038/s41589-020-0529-6. [PubMed: 32367017]
- Ma X, He D, Ru X, Chen Y, Cai Y, Bruce IC, Xia Q, Yao X, and Jin J (2012). Apigenin, a plant-derived flavone, activates transient receptor potential vanilloid 4 cation channel. *Br. J. Pharmacol* 166, 349–358. 10.1111/j.1476-5381.2011.01767.x. [PubMed: 22049911]
- Mason RP, Jacob RF, Shrivastava S, Sherratt SCR, and Chattopadhyay A (2016). Eicosapentaenoic acid reduces membrane fluidity, inhibits cholesterol domain formation, and normalizes bilayer width in atherosclerotic-like model membranes. *Biochim. Biophys. Acta* 1858, 3131–3140. 10.1016/j.bbamem.2016.10.002. [PubMed: 27718370]
- Monaghan K, McNaughten J, McGahon MK, Kelly C, Kyle D, Yong PH, McGeown JG, and Curtis TM (2015). Hyperglycemia and diabetes downregulate the functional expression of TRPV4 channels in retinal microvascular endothelium. *PLoS One* 10, e0128359. 10.1371/journal.pone.0128359. [PubMed: 26047504]
- Ossani GP, Denninghoff VC, Uceda AM, Díaz ML, Uicich R, and Monserrat AJ (2015). Short-term menhaden oil rich diet changes renal lipid profile in acute kidney injury. *J. Oleo Sci* 64, 497–503. 10.5650/jos.ess14186. [PubMed: 25948137]
- Ottolini M, Hong K, Cope EL, Daneva Z, DeLalio LJ, Sokolowski JD, Marziano C, Nguyen NY, Altschmied J, Haendeler J, et al. (2020). Local peroxynitrite impairs endothelial transient receptor potential vanilloid 4 channels and elevates blood pressure in obesity. *Circulation* 141, 1318–1333. 10.1161/CIRCULATIONAHA.119.043385. [PubMed: 32008372]
- Pankey EA, Zsombok A, Lasker GF, and Kadowitz PJ (2014). Analysis of responses to the TRPV4 agonist GSK1016790A in the pulmonary vascular bed of the intact-chest rat. *Am. J. Physiol. Heart Circ. Physiol* 306, H33–H40. 10.1152/ajpheart.00303.2013. [PubMed: 24186096]
- Peixoto-Neves D, Wang Q, Leal-Cardoso JH, Rossoni LV, and Jaggar JH (2015). Eugenol dilates mesenteric arteries and reduces systemic BP by activating endothelial cell TRPV4 channels. *Br. J. Pharmacol* 172, 3484–3494. 10.1111/bph.13156. [PubMed: 25832173]
- Randall AS, Liu CH, Chu B, Zhang Q, Dongre SA, Juusola M, Franze K, Wakelam MJO, and Hardie RC (2015). Speed and sensitivity of phototransduction in *Drosophila* depend on degree of saturation of membrane phospholipids. *J. Neurosci* 35, 2731–2746. 10.1523/JNEUROSCI.1150-14.2015. [PubMed: 25673862]
- Ridone P, Grage SL, Patkunarajah A, Battle AR, Ulrich AS, and Martinac B (2018). “Force-from-lipids” gating of mechanosensitive channels modulated by PUFAs. *J. Mech. Behav. Biomed. Mater* 79, 158–167. 10.1016/j.jmbbm.2017.12.026. [PubMed: 29304430]
- Ridone P, Pandzic E, Vassalli M, Cox CD, Macmillan A, Gottlieb PA, and Martinac B (2020). Disruption of membrane cholesterol organization impairs the activity of PIEZO1 channel clusters. *J. Gen. Physiol* 152, e201912515. 10.1085/jgp.201912515. [PubMed: 32582958]
- Romero LO, Massey AE, Mata-Daboín AD, Sierra-Valdez FJ, Chauhan SC, Cordero-Morales JF, and Vásquez V (2019). Dietary fatty acids fine-tune Piezo1 mechanical response. *Nat. Commun* 10, 1200. 10.1038/s41467-019-09055-7. [PubMed: 30867417]
- Seki T, Goto K, Kiyohara K, Kansui Y, Murakami N, Haga Y, Ohtsubo T, Matsumura K, and Kitazono T (2017). Downregulation of endothelial transient receptor potential vanilloid type 4 channel and small-conductance of Ca²⁺-activated K⁺ channels underpins impaired endothelium-dependent hyperpolarization in hypertension. *Hypertension* 69, 143–153. 10.1161/HYPERTENSIONAHA.116.07110. [PubMed: 27872234]

- Shamsaldeen YA, Lione LA, and Benham CD (2020). Dysregulation of TRPV4, eNOS and caveolin-1 contribute to endothelial dysfunction in the streptozotocin rat model of diabetes. *Eur. J. Pharmacol* 888, 173441. 10.1016/j.ejphar.2020.173441. [PubMed: 32810492]
- Simopoulos AP (2016). An increase in the omega-6/omega-3 fatty acid ratio increases the risk for obesity. *Nutrients* 8, 128. 10.3390/nu8030128. [PubMed: 26950145]
- Sonkusare SK, Bonev AD, Ledoux J, Liedtke W, Kotlikoff MI, Heppner TJ, Hill-Eubanks DC, and Nelson MT (2012). Elementary Ca²⁺ signals through endothelial TRPV4 channels regulate vascular function. *Science* 336, 597–601. 10.1126/science.1216283. [PubMed: 22556255]
- Strotmann R, Harteneck C, Nunnenmacher K, Schultz G, and Plant TD (2000). OTRPC4, a nonselective cation channel that confers sensitivity to extracellular osmolarity. *Nat. Cell Biol* 2, 695–702. 10.1038/35036318. [PubMed: 11025659]
- Swanson D, Block R, and Mousa SA (2012). Omega-3 fatty acids EPA and DHA: health benefits throughout life. *Adv. Nutr* 3, 1–7. 10.3945/an.111.000893. [PubMed: 22332096]
- Takahashi N, Hamada-Nakahara S, Itoh Y, Takemura K, Shimada A, Ueda Y, Kitamata M, Matsuoka R, Hanawa-Suetsugu K, Senju Y, et al. (2014). TRPV4 channel activity is modulated by direct interaction of the ankyrin domain to PI(4, 5)P(2). *Nat. Commun* 5, 4994. 10.1038/ncomms5994. [PubMed: 25256292]
- Thorneloe KS, Sulpizio AC, Lin Z, Figueroa DJ, Clouse AK, McCafferty GP, Chendrimada TP, Lashinger ESR, Gordon E, Evans L, et al. (2008). N-((1S)-1-[[4-((2S)-2-[[2, 4-dichlorophenyl)sulfonyl]amino]-3-hydroxypropanoyl]-1-piperazinyl]carbonyl)-3-methylbutyl)-1-benzothiophene-2-carboxamide (GSK1016790A), a novel and potent transient receptor potential vanilloid 4 channel agonist induces urinary bladder contraction and hyperactivity: Part I. *J. Pharmacol. Exp. Ther* 326, 432–442. 10.1124/jpet.108.139295. [PubMed: 18499743]
- Tousoulis D, Plastiras A, Siasos G, Oikonomou E, Verveniotis A, Kokkou E, Maniatis K, Gouliopoulos N, Miliou A, Paraskevopoulos T, and Stefanadis C (2014). Omega-3 PUFAs improved endothelial function and arterial stiffness with a parallel antiinflammatory effect in adults with metabolic syndrome. *Atherosclerosis* 232, 10–16. 10.1016/j.atherosclerosis.2013.10.014. [PubMed: 24401211]
- Vriens J, Owsianik G, Fisslthaler B, Suzuki M, Janssens A, Voets T, Morisseau C, Hammock BD, Fleming I, Busse R, and Nilius B (2005). Modulation of the Ca²⁺ permeable cation channel TRPV4 by cytochrome P450 epoxygenases in vascular endothelium. *Circ. Res* 97, 908–915. 10.1161/01.RES.0000187474.47805.30. [PubMed: 16179585]
- Vriens J, Watanabe H, Janssens A, Droogmans G, Voets T, and Nilius B (2004). Cell swelling, heat, and chemical agonists use distinct pathways for the activation of the cation channel TRPV4. *Proc. Natl. Acad. Sci. USA* 101, 396–401. 10.1073/pnas.0303329101. [PubMed: 14691263]
- Wallis JG, Watts JL, and Browse J (2002). Polyunsaturated fatty acid synthesis: what will they think of next? *Trends Biochem. Sci* 27, 467. [PubMed: 12217522]
- Watanabe H, Davis JB, Smart D, Jerman JC, Smith GD, Hayes P, Vriens J, Cairns W, Wissenbach U, Prenen J, et al. (2002a). Activation of TRPV4 channels (hVRL-2/mTRP12) by phorbol derivatives. *J. Biol. Chem* 277, 13569–13577. 10.1074/jbc.M200062200. [PubMed: 11827975]
- Watanabe H, Vriens J, Suh SH, Benham CD, Droogmans G, and Nilius B (2002b). Heat-evoked activation of TRPV4 channels in a HEK293 cell expression system and in native mouse aorta endothelial cells. *J. Biol. Chem* 277, 47044–47051. 10.1074/jbc.M208277200. [PubMed: 12354759]
- Watts JL, and Browse J (2002). Genetic dissection of polyunsaturated fatty acid synthesis in *Caenorhabditis elegans*. *Proc. Natl. Acad. Sci. USA* 99, 5854–5859. 10.1073/pnas.092064799. [PubMed: 11972048]
- White JPM, Cibelli M, Urban L, Nilius B, McGeown JG, and Nagy I (2016). TRPV4: molecular conductor of a diverse orchestra. *Physiol. Rev* 96, 911–973. 10.1152/physrev.00016.2015. [PubMed: 27252279]
- Wiest EF, Walsh-Wilcox MT, Rothe M, Schunck WH, and Walker MK (2016). Dietary omega-3 polyunsaturated fatty acids prevent vascular dysfunction and attenuate cytochrome P4501A1 expression by 2, 3, 7, 8-Tetrachlorodibenzo-p-dioxin. *Toxicol. Sci* 154, 43–54. 10.1093/toxsci/kfw145. [PubMed: 27492226]

- Willette RN, Bao W, Nerurkar S, Yue TL, Doe CP, Stankus G, Turner GH, Ju H, Thomas H, Fishman CE, et al. (2008). Systemic activation of the transient receptor potential vanilloid subtype 4 channel causes endothelial failure and circulatory collapse: Part 2. *J. Pharmacol. Exp. Ther* 326, 443–452. 10.1124/jpet.107.134551. [PubMed: 18499744]
- Wissenbach U, Bödding M, Freichel M, and Flockerzi V (2000). Trp12, a novel Trp related protein from kidney. *FEBS Lett.* 485, 127–134. [PubMed: 11094154]
- Xu H, Fu Y, Tian W, and Cohen DM (2006). Glycosylation of the osmoresponsive transient receptor potential channel TRPV4 on Asn-651 influences membrane trafficking. *Am. J. Physiol. Renal Physiol* 290, F1103–F1109. 10.1152/ajprenal.00245.2005. [PubMed: 16368742]
- Zhang X, Mao A, Xiao W, Zhang P, Han X, Zhou T, Chen Y, Jin J, and Ma X (2019). Morin induces endothelium-dependent relaxation by activating TRPV4 channels in rat mesenteric arteries. *Eur. J. Pharmacol* 859, 172561. 10.1016/j.ejphar.2019.172561. [PubMed: 31326379]

Highlights

- EPA increases TRPV4 activity in human endothelial cells of various vascular beds
- Dietary or genetic enrichment of EPA enhances TRPV4-mediated vasodilation in mice
- EPA decreases Ca²⁺-dependent TRPV4 desensitization
- TRPV4 N terminus is required for EPA-mediated reduction in channel desensitization

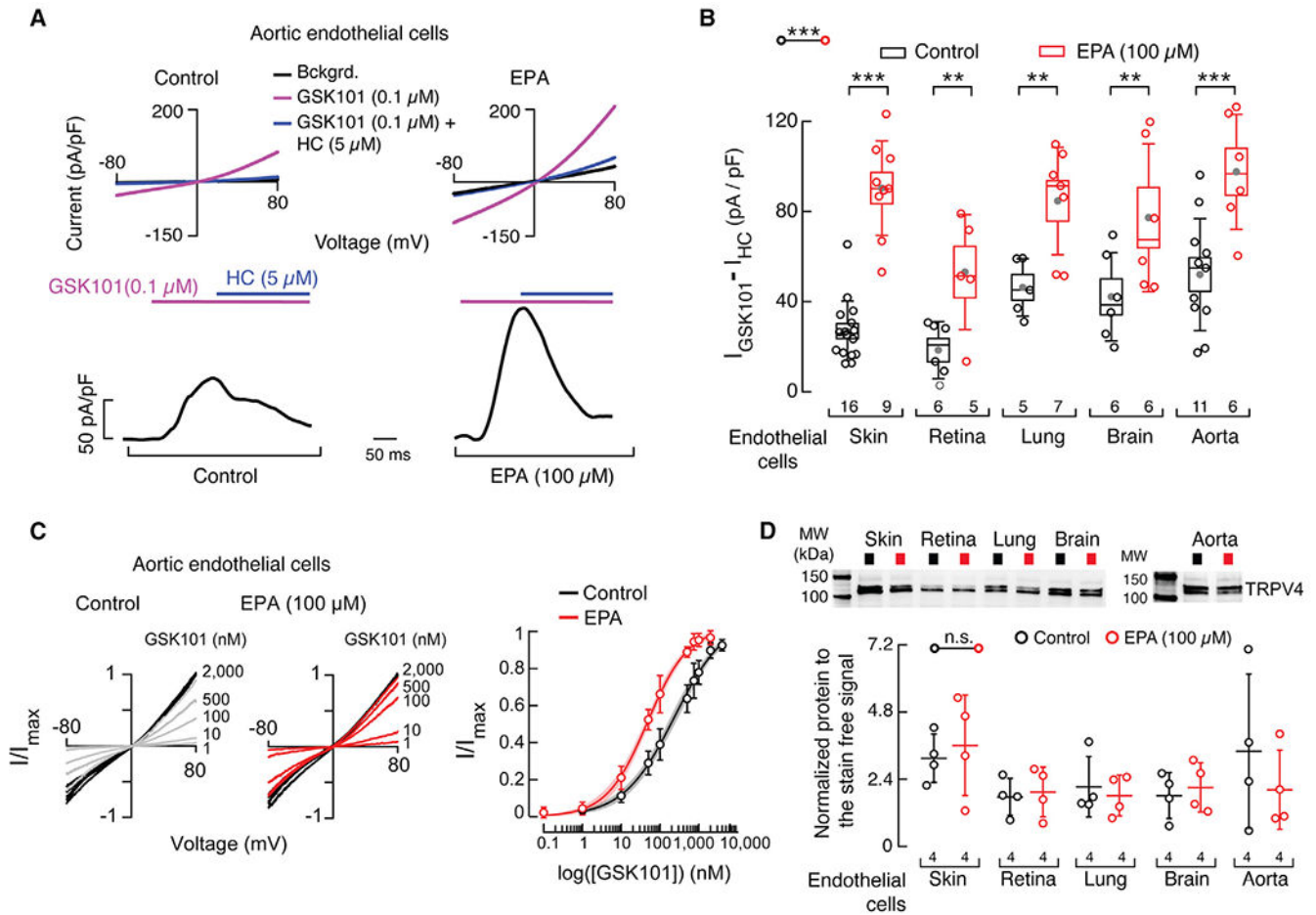


Figure 1. EPA supplementation enhances TRPV4 activity in primary human vascular endothelial cells

(A) Top: representative current-voltage relationships determined by whole-cell patch-clamp recordings of control and EPA (100 μ M)-treated aortic endothelial cells challenged with GSK1016790A (GSK101, TRPV4 agonist, 0.1 μ M) and GSK101 (0.1 μ M) + HC067047 (HC, TRPV4 antagonist; 5 μ M). Bckgrd. indicates background currents. Bottom: representative time course of whole-cell patch-clamp recordings (+80 mV) of control and EPA-treated aortic endothelial cells challenged with GSK101 and inhibited with HC.

(B) Boxplots show the mean (gray circle), median (bisecting line), SD (whiskers), and SEM (box) of TRPV4 currents ($I_{GSK101} - I_{HC}$) pA/pF obtained by whole-cell patch-clamp recordings (+80 mV) of control and EPA-treated endothelial cells from skin, retina, lung, brain, and aorta. Two-way ANOVA and Sidak-Holm multiple comparisons test.

(C) Left: representative current-voltage relationships determined by whole-cell patch-clamp recordings of control and EPA (100 μ M)-treated aortic endothelial cells challenged with GSK101 (from 1 to 2,000 nM). Currents evoked by GSK101 submaximal concentrations (gray and red traces) were normalized by corresponding currents elicited by saturating GSK101 (2,000 nM; black traces) per cell. Right: normalized (I/I_{max}) GSK101 dose-response profiles of control and EPA (100 μ M)-treated aortic endothelial cells. A Hill function was fitted to the data. The shadows encompassing the curves indicate the 95%

confidence bands for the fit. Circles are mean \pm SD. n = 36 for control and n = 36 for EPA (100 μ M)-treated aortic endothelial cells.

(D) Top: representative western blots (anti-TRPV4) of the membrane fractions of control and EPA (100 μ M)-treated human endothelial cells from skin, retina, lung, brain, and aorta. Bottom: mean/scatter-dot plot showing relative intensities of TRPV4 bands, calculated from total protein detection of chemically labeled proteins (Stain-Free System Bio-Rad), from the membrane fractions of control and EPA (100 μ M)-treated endothelial cells. Lines are mean \pm SD. Two-way ANOVA. Asterisks indicate values significantly different from control (***p < 0.001 and **p < 0.01) and n.s. indicates values not significantly different from the control. n is indicated in each panel. See also Figures S1 and S2.

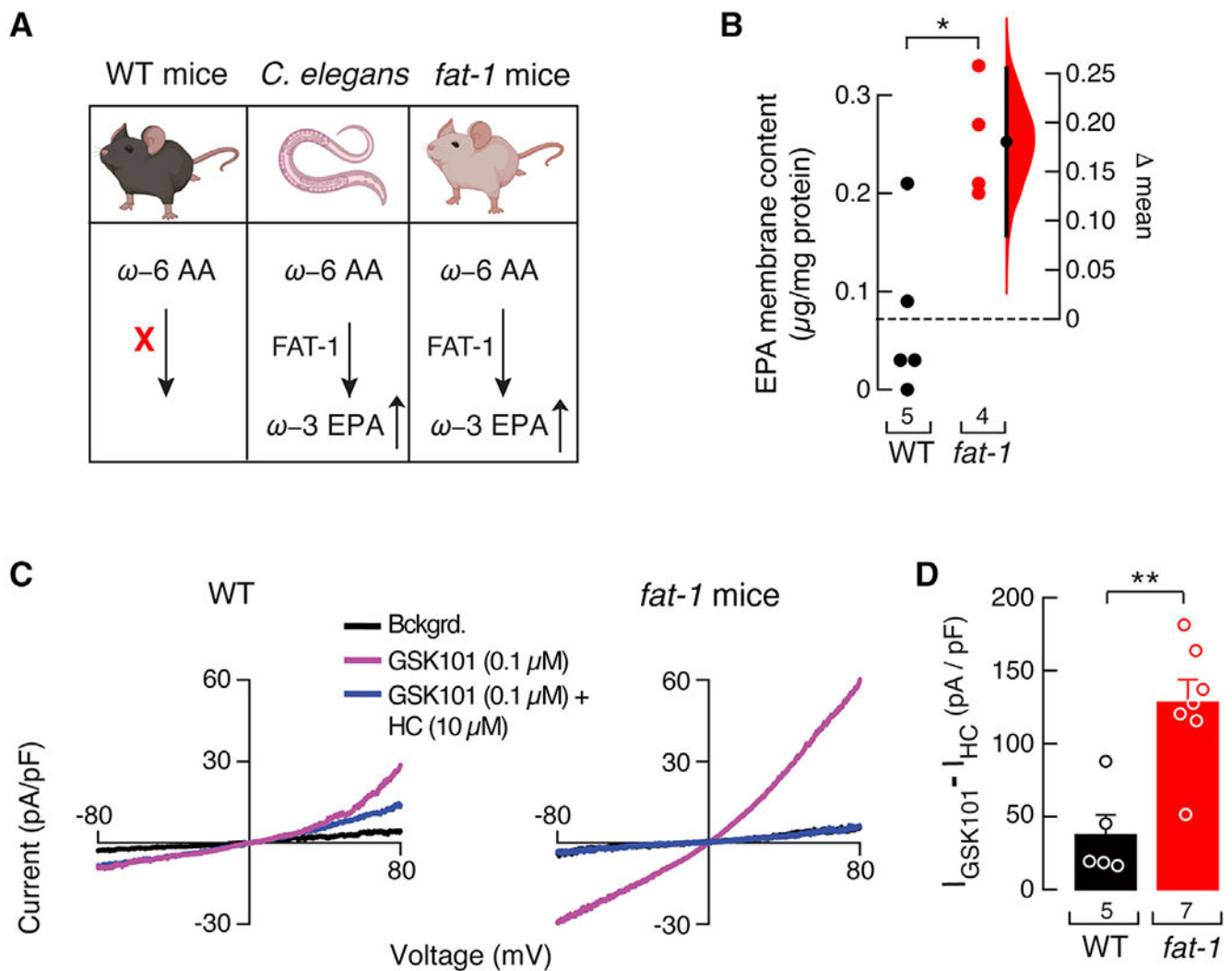


Figure 2. Isolated endothelial cells from *fat-1* mice have increased TRPV4 activity

(A) The *C. elegans* fatty acid desaturase FAT-1 enzyme introduces a double bond in ω -6 arachidonic acid to synthesize ω -3 EPA in worms and transgenic *fat-1* mice, but not in WT mice. Mice and *C. elegans* cartoons were created with [BioRender.com](https://www.biorender.com).

(B) Gardner-Altman estimation plot showing the mean difference in EPA-membrane content of whole mesenteric arteries of WT and *fat-1* mice, as determined by LC-MS. The raw data are plotted on the left axis. The mean difference, on the right, is depicted as a dot; the 95% confidence interval is indicated by the ends of the vertical error bars. Mann-Whitney rank test for two independent groups.

(C) Representative current-voltage relationships determined by whole-cell patch-clamp recordings of WT and *fat-1* cultured isolated mesenteric endothelial cells challenged with GSK101 (0.1 μ M) and GSK101 (0.1 μ M) + HC (10 μ M). Bckgrd. indicates background currents.

(D) Bar graph displaying TRPV4 currents ($I_{\text{GSK101}} - I_{\text{HC}}$) pA/pF obtained by whole-cell patch-clamp recordings (+80 mV) of cultured isolated mesenteric endothelial cells of WT

and *fat-1* mice. Bars are mean \pm SEM. Two-tailed unpaired t test. Asterisks indicate values significantly different from WT (**p < 0.01 and *p < 0.05). n is indicated in each panel.

Author Manuscript

Author Manuscript

Author Manuscript

Author Manuscript

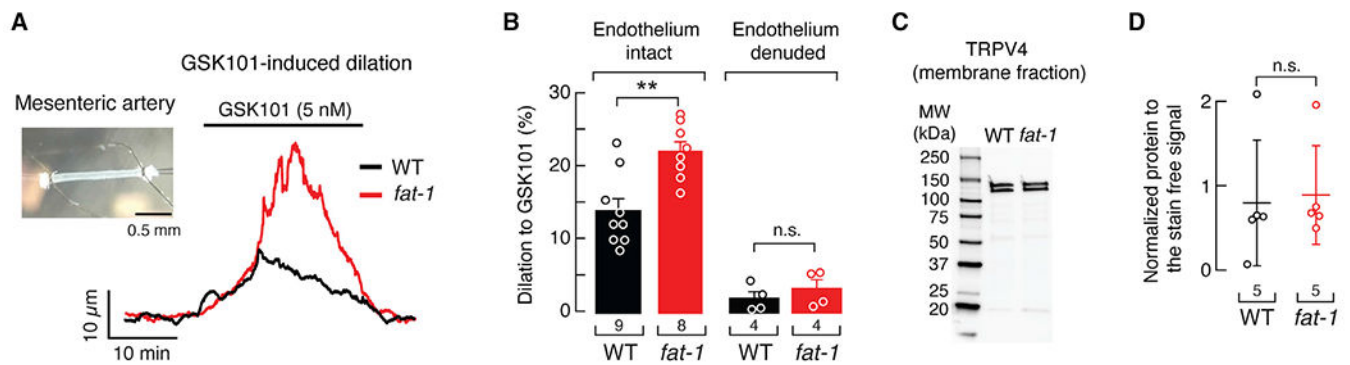


Figure 3. Mesenteric arteries from *fat-1* mice display enhanced TRPV4-mediated vasodilation
 (A) Representative time course of GSK101 (5 nM)-induced vasodilation of pressurized (80 mmHg) mesenteric arteries from WT and *fat-1* mice. Inset: micrograph of a representative cannulated mesenteric artery.
 (B) Percentage of GSK101 (5 nM)-induced vasodilation of mesenteric arteries (endothelium-intact or -denuded) from WT and *fat-1* mice. Bars are mean \pm SEM. Two-way ANOVA and Tukey multiple comparisons test.
 (C) Representative western blot (anti-TRPV4) of the membrane fractions of WT and *fat-1* mice mesenteric arteries.
 (D) Mean/scatter-dot plot showing relative intensities of TRPV4 bands, calculated from total protein detection of chemically labeled proteins (Stain-Free System Bio-Rad), from the membrane fractions of mesenteric arteries from WT and *fat-1* mice. Lines are mean \pm SD. Two-tailed unpaired t test. Asterisks indicate values significantly different from WT (** $p < 0.01$) and n.s. indicates values not significantly different from the WT. n is indicated in each panel. See also Figure S3.

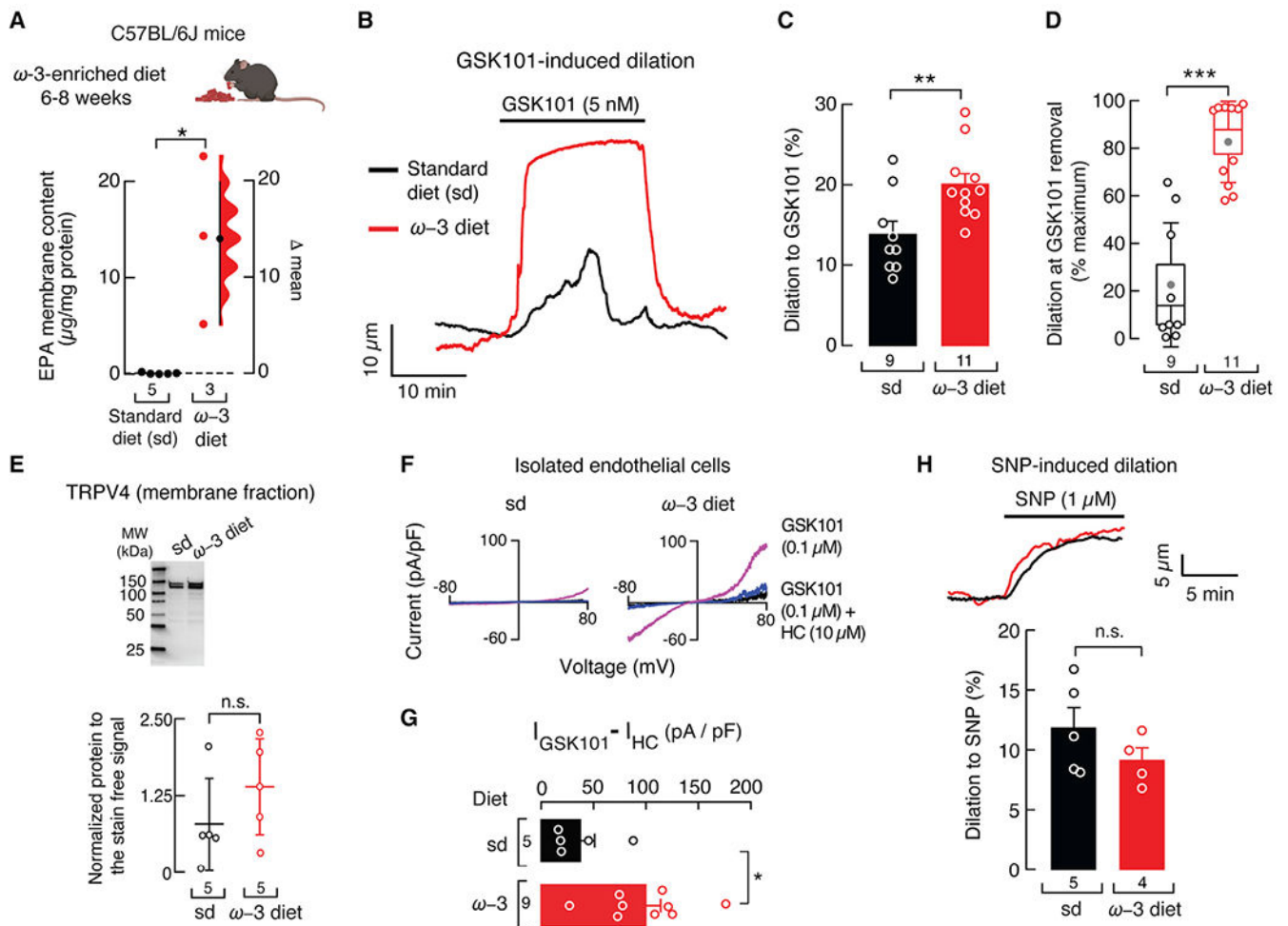


Figure 4. An ω-3 enriched diet increases TRPV4-mediated vasodilation in WT mice

(A) Gardner-Altman estimation plot showing the mean difference in EPA-membrane content of whole mesenteric arteries of WT mice fed with standard or ω-3 fatty acid-enriched diets, as determined by LC-MS. The raw data are plotted on the left axis. The mean difference, on the right, is depicted as a dot; the 95% confidence interval is indicated by the ends of the vertical error bars. Mann-Whitney rank test for two independent groups. Mouse cartoon was created with [BioRender.com](https://www.biorender.com).

(B) Representative time course of GSK101 (5 nM)-induced vasodilation of pressurized (80 mmHg) mesenteric arteries from WT mice fed with standard or ω-3 fatty acid-enriched diets.

(C) Percentage of GSK101 (5 nM)-induced vasodilation of mesenteric arteries from WT mice fed with standard or ω-3 fatty acid-enriched diets. Bars are mean ± SEM. Two-tailed unpaired t test.

(D) Boxplots show the mean (gray circle), median (bisecting line), SD (whiskers), and SEM (box) of the percentage of maximal GSK101 (5 nM)-induced vasodilation remaining at the time GSK101 was removed from the mesenteric arteries of WT mice fed with standard or ω-3 fatty acid-enriched diets. Two-tailed unpaired t test.

(E) Top: representative western blot (TRPV4) from membrane fractions of the mesenteric arteries from WT mice fed with standard or ω -3 fatty acid-enriched diets. Bottom: mean/scatter-dot plot showing relative intensities of TRPV4 bands, calculated from total protein detection of chemically labeled proteins (Stain-Free System Bio-Rad), from the membrane fractions of mesenteric arteries from WT mice fed with standard or ω -3 fatty acid-enriched diets. Lines are mean \pm SD. Two-tailed unpaired t test.

(F) Representative current-voltage relationships determined by whole-cell patch-clamp recordings of cultured isolated mesenteric endothelial cells, from WT mice fed with standard or ω -3 fatty acid-enriched diets, challenged with GSK101 (0.1 μ M) and GSK101 (0.1 μ M) + HC (10 μ M).

(G) Bar graph displaying TRPV4 currents ($I_{\text{GSK101}} - I_{\text{HC}}$) pA/pF obtained by whole-cell patch-clamp recordings (+80 mV) of cultured isolated mesenteric endothelial cells of WT mice fed with standard or ω -3 fatty acid-enriched diets. Bars are mean \pm SEM. Two-tailed unpaired t test.

(H) Top: representative time course of sodium nitroprusside (SNP) (1 μ M)-induced vasodilation of pressurized (80 mmHg) mesenteric arteries from WT mice fed with standard or ω -3 fatty acid-enriched diets. Bottom: percentage of SNP (1 μ M)-induced vasodilation of WT mice fed with standard or ω -3 fatty acid-enriched diets. Bars are mean \pm SEM. Two-tailed unpaired t test. Asterisks indicate values significantly different from standard diet (** $p < 0.001$, ** $p < 0.01$, and * $p < 0.05$) and n.s. indicates values not significantly different from the standard diet. n is indicated in each panel. See also Figure S4.

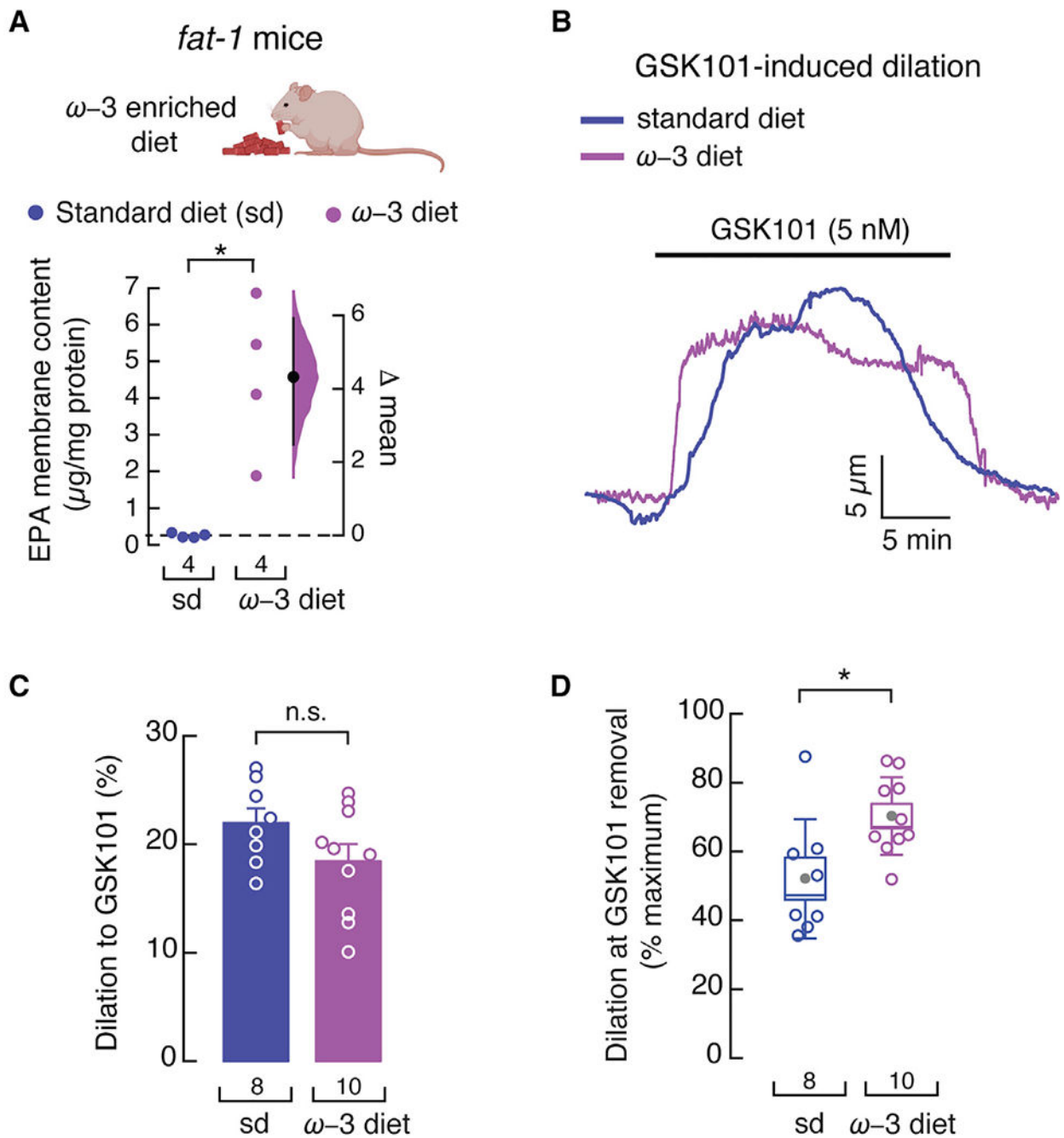


Figure 5. An ω -3 enriched diet decreases TRPV4-mediated vasodilation decay in *fat-1* mouse arteries

(A) Gardner-Altman estimation plot showing the mean difference in EPA-membrane content of whole mesenteric arteries from *fat-1* mice fed with standard or ω -3 fatty acid-enriched diets, as determined by LC-MS. The raw data are plotted on the left axis. The mean difference, on the right, is depicted as a dot; the 95% confidence interval is indicated by the ends of the vertical error bars. n is denoted below the circles. Mann-Whitney rank test for two independent groups. Mouse cartoon was created with [BioRender.com](https://www.biorender.com).

(B) Representative time course of GSK101 (5 nM)-induced vasodilation of pressurized (80 mmHg) mesenteric arteries from *fat-1* mice fed with standard or ω -3 fatty acid-enriched diets.

(C) Percentage of GSK101 (5 nM)-induced vasodilation of mesenteric arteries from *fat-1* mice fed with standard or ω -3 fatty acid-enriched diets. Bars are mean \pm SEM. Two-tailed unpaired t test.

(D) Boxplots show the mean (gray circle), median (bisecting line), SD (whiskers), and SEM (box) of the percentage of maximal GSK101 (5 nM)-induced vasodilation remaining at the time GSK101 was removed from the mesenteric arteries of *fat-1* mice fed with standard or ω -3 fatty acid-enriched diets. Two-tailed unpaired t test. Asterisks indicate values significantly different from the standard diet (* $p < 0.05$) and n.s. indicates values not significantly different from the standard diet. n is indicated in each panel. See also Figure S5.

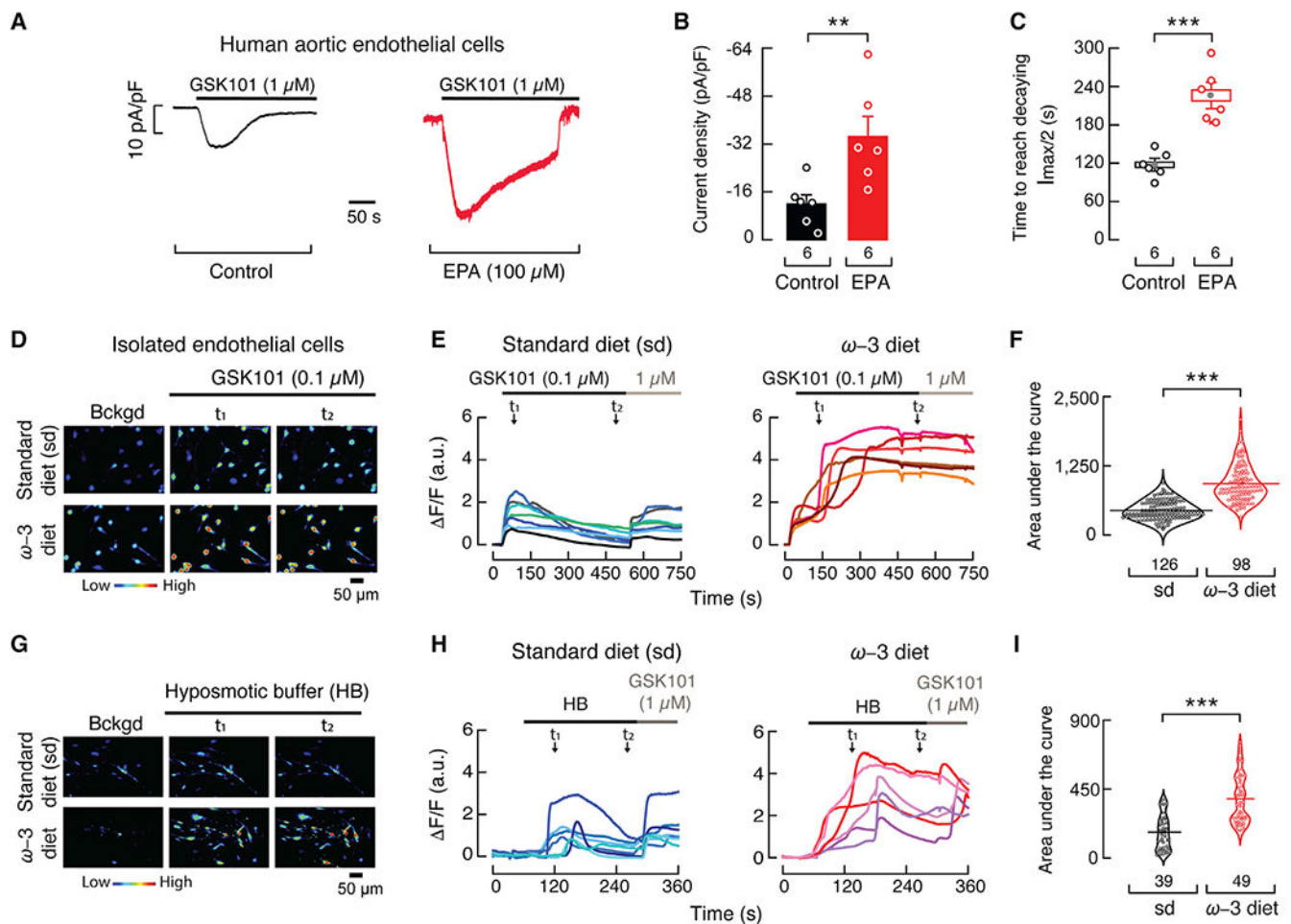


Figure 6. EPA supplementation decreases TRPV4 desensitization

(A) Representative time course of whole-cell patch-clamp recordings (-60 mV) of control and EPA (100 μM)-treated human aortic endothelial cells challenged with GSK101 (1 μM). (B) Bar graph displaying TRPV4 currents (pA/pF) obtained by whole-cell patch-clamp recordings (-60 mV) of control and EPA (100 μM)-treated aortic endothelial cells. Bars are mean \pm SEM. Mann-Whitney rank test for two independent groups. (C) Boxplots show mean (gray circle), median (bisecting line), SD (whiskers), and SEM (box) of the time to reach half amplitude from the peak current (I_{max}) elicited by GSK101 (1 μM) in control and EPA (100 μM)-treated aortic endothelial cells. Two-tailed unpaired t test.

(D) Micrographs of cultured isolated mesenteric endothelial cells from WT mice fed with standard or ω -3 fatty acid-enriched diets, loaded with Fluo-4 AM, and challenged with GSK101 (0.1 μM). The color bar indicates a relative change in fluorescence intensity. Experiments were performed in three independent cell preparations. t indicates the times at which representative micrographs were taken from the traces in (E).

(E) Representative traces corresponding to normalized intensity changes ($\Delta F/F$) of individual cells shown in (D).

(F) Area under the curve (AUC) of the fluorescence response (F/F), depicted as violin plots with the means shown as horizontal bars, of endothelial cells from WT mice fed with standard or ω -3 fatty acid-enriched diets challenged with GSK101. Two-tailed unpaired t test.

(G) Micrographs of cultured isolated mesenteric endothelial cells of WT mice fed with standard or ω -3 fatty acid-enriched diets, loaded with Fluo-4 AM and challenged with a hypoosmotic buffer (HB: 240 mOsm). The color bar indicates a relative change in fluorescence intensity. Experiments were performed in two independent cell preparations. t indicates the times at which representative micrographs were taken from the traces in (H).

(H) Representative traces corresponding to normalized intensity changes (F/F) of individual cells shown in (G).

(I) AUC of the fluorescence response (F/F), depicted as violin plots with the means shown as horizontal bars, of endothelial cells from WT mice fed with standard or ω -3 fatty acid-enriched diets challenged with a hypoosmotic buffer. Two-tailed unpaired t test. Asterisks indicate values significantly different from control or standard diet (** $p < 0.001$ and ** $p < 0.01$). n is indicated in each panel.

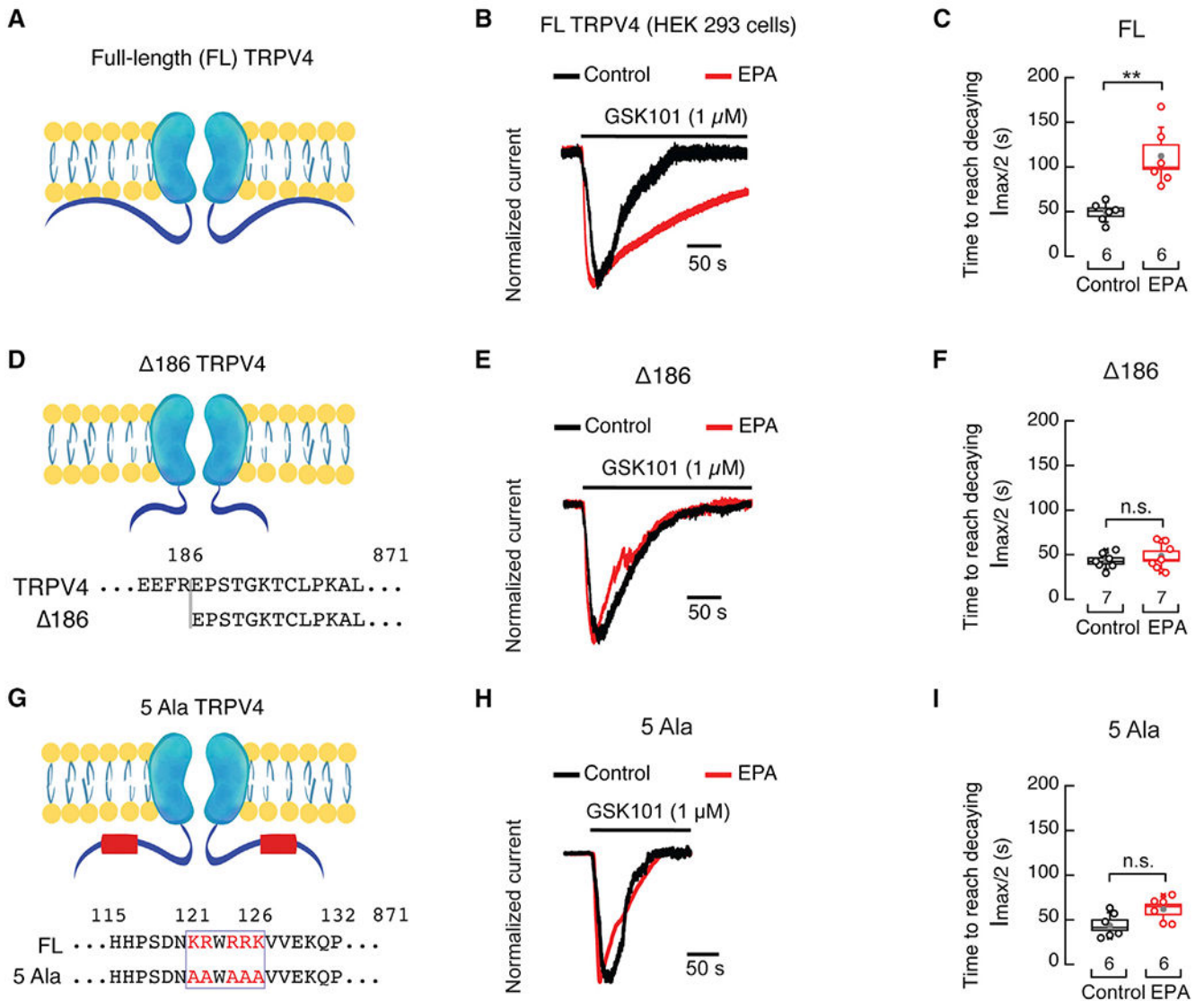


Figure 7. TRPV4 proximal N terminus determines the effect of EPA on desensitization

(A) Cartoon depicting the full-length rat TRPV4 channel.

(B) Representative time course of whole-cell patch-clamp recordings (-60 mV) of control and EPA (100 μ M)-treated HEK293 cells, expressing full-length rat TRPV4, challenged with GSK101 (1 μ M). Traces were normalized for comparison.

(C) Boxplots show mean (gray circle), median (bisecting line), SD (whiskers), and SEM (box) of the time to reach half amplitude from the peak current (I_{max}) elicited by GSK101 (1 μ M) in control and EPA (100 μ M)-treated HEK293 cells expressing full-length rat TRPV4. Two-tailed unpaired with Welch's correction.

(D) Cartoon depicting the Δ 186 rat TRPV4 channel construct.

(E) Representative time course of whole-cell patch-clamp recordings (-60 mV) of control and EPA (100 μ M)-treated HEK293 cells, expressing the Δ 186 rat TRPV4 channel construct, challenged with GSK101 (1 μ M). Traces were normalized for comparison.

(F) Boxplots show mean (gray circle), median (bisecting line), SD (whiskers), and SEM (box) of the time to reach half amplitude from the peak current (I_{max}) elicited by GSK101 (1 μ M) in control and EPA (100 μ M)-treated HEK293 cells expressing the 186 rat TRPV4 channel construct. Two-tailed unpaired t test.

(G) Cartoon depicting the 5Ala (K121A, R122A, R124A, R125A, K126A) rat TRPV4 channel construct.

(H) Representative time course of whole-cell patch-clamp recordings (-60 mV) in control and EPA (100 μ M)-treated HEK293 cells expressing the 5Ala rat TRPV4 channel construct challenged with GSK101 (1 μ M). Traces were normalized for comparison.

(I) Boxplots show mean (gray circle), median (bisecting line), SD (whiskers), and SEM (box) of the time to reach half amplitude from the peak current (I_{max}) elicited by GSK101 (1 μ M) of control and EPA (100 μ M)-treated HEK293 cells expressing the 5Ala rat TRPV4 channel construct. Two-tailed unpaired t test. Asterisks indicate values significantly different from control (** $p < 0.01$) and n.s. indicates values not significantly different from the control. n is indicated in each panel. See also Figure S5.

KEY RESOURCES TABLE

REAGENT or RESOURCE	SOURCE	IDENTIFIER
Antibodies		
Rabbit polyclonal anti-human TRPV4	Abcepta	Cat# AP18990a, RRID: AB_2923215
Goat anti-rabbit IgG HL-HRP conjugated	Bio-Rad	Cat# 170-6515, RRID: AB_11125142
Biological samples		
Mouse mesenteric arteries (third and fourth order)	This study	N/A
Chemicals, peptides, and recombinant proteins		
Sodium Chloride	Fisher Scientific	S271-500
Potassium Chloride	Fisher Scientific	P217-500
Magnesium Chloride	Fisher Scientific	BP214-500
Glucose	Sigma	G8270-1KG
HEPES	Fisher Scientific	BP310-100
Calcium Chloride	Fisher Scientific	C78-500
Cesium Chloride	Acros	7647-17-8
Sodium Bicarbonate	Fisher Scientific	S233-3
Magnesium Sulfate	Fisher Scientific	BP213-1
Potassium Dihydrogen Phosphate	Fisher Scientific	P285-500
EGTA	Fisher Scientific	O2783-100
Sodium Hydroxide	Fisher Scientific	SS266-1
Cesium Hydroxide	Acros	35103-79-8
Lipofectamine 2000	Fisher Scientific	O2783-100
Opti-MEM	Invitrogen	52887
DMEM	Gibco	11965-092
Fetal Bovine Serum	Gibco	11965-092
Penicillin-Streptomycin	Gibco	10082-147
Trypsin	Santa Cruz	25055-82-7
Pluronic F127	Millipore Sigma	30525-89-4
Fluo4-AM	Fisher Scientific	F14201
Collagenase Type 2	Worthington	LS004196
Isoflurane	Baxter	10019-360-60

REAGENT or RESOURCE	SOURCE	IDENTIFIER
Menhaden oil supplemented mouse diet	Dyets Inc	112246
Standard mouse diet	Envigo	Teklad LM-485
Eicosapentaenoic acid (C20:5)	Nu-Check Prep	U-99-A
GSK1016790A	Sigma-Aldrich	G0798
HC067047	Sigma-Aldrich	SML0143
Dulbecco's Phosphate Buffered Solution (DPBS)	Gibco	14190-144
Complete Clasic Medium	Cell Systems	4Z0-500
Endothelial Cell Growth Medium MV 2	Promo Cell	C-22121
Halt Protease Inhibitor Cocktail	Fisher Scientific	1861281
Passage Reagent System	Cell Systems	4Z0-840
Bac-Off Antibiotic	Cell Systems	4Z0-644
Mini-PROTEAN TGX Stain-Free Precast Gels (4-15%, 50 µl)	Bio-Rad	4568084
Clarity Max Western ECL Substrate	Bio-Rad	1705062
Dyclonine hydrochloride	Sigma-Aldrich	1230000
2-APB	Tocris	1224
Capsazepine	Tocris	464
(E)-Capsaicin	Tocris	462
Allyl isothiocyanate	Sigma-Aldrich	377430
HC-030031	Sigma-Aldrich	H4415
GSK 1702934A	Tocris	6508
GSK 2833503A	Tocris	6497
Critical commercial assays		
Mem-PER™ Plus Membrane Protein Extraction Kit	ThermoFisher	89842
Deposited Data		
Individual data deposit	Figshare	10.6084/m9.figshare.16692073
Experimental models: Cell lines		
Primary Human Dermal Microvascular Endothelial Cells	Cell Systems	CSC 2M1
Primary Human Retinal Microvascular Endothelial Cells	Cell Systems	ACBRI181
Primary Human Lung Microvascular Endothelial Cells	Cell Systems	ACBRI468
Primary Human Brain Microvascular Endothelial Cells	Cell Systems	ACBRI376
Primary Human Aortic Endothelial Cells	Cell Systems	ACBRI375
Human: HEK293	ATCC	CRL-1573
Experimental models: Organisms/strains		
C57BL/6J mice	The Jackson Laboratory	000664

REAGENT or RESOURCE	SOURCE	IDENTIFIER
C57BL/6-Tg(CAG- <i>fat-1</i>)1Jxkx/J mice	The Jackson Laboratory	020097
Oligonucleotides		
186 TRPV4 Fw (rTRPV4-186-BamHI-Fw): 5'-CGGGGATCCATGGAACCATCCACAGGGAAGACC-3'	Life Technologies	NA
186 TRPV4 Rv (rTRPV4NotIRv): 5'-GCGGAGGACGCACCACTGTAGGCGGCCGCGGGCCC-3'	Life Technologies	NA
TRPV4_121-122-124-125-126A Fw: 5'-TACCGGCACCACCCAGTGACAACGCGGCATGGGCGGGGGCGGTGCGAGAAGCAGCCACAGAG-3'	Invitrogen	458479F01
TRPV4_121-122-124-125-126A Rv: 5'-CTCTGTGGCTGCTTCTCTACGACCGCCGCCCATGCCGCGTTGTCACTGGGGTGGTGCCGGTC-3'	Invitrogen	458479F02
Recombinant DNA		
Plasmid: rat <i>Trpv4</i> pMO	Laboratory of Julio Cordero-Morales	N/A
Plasmid: rat <i>Trpv4</i> 186 pMO	Laboratory of Julio Cordero-Morales	N/A
Plasmid: <i>GFP</i> pMO	Laboratory of Julio Cordero-Morales	N/A
Plasmid: rat <i>Trpv4</i> 5Ala (121-122-124-125-126A) pMO	Laboratory of Julio Cordero-Morales	N/A
Software and algorithms		
IonWizard	Ionoptix	https://www.ionoptix.com/
ImageLab	Bio-Rad	https://www.bio-rad.com
Clampfit 10.4	Molecular Devices	https://www.moleculardevices.com/
Clampex 10.5	Molecular Devices	https://www.moleculardevices.com/
Origin 2018	OriginLab	https://www.originlab.com/
GraphPad instant 3	Dotmatics	https://www.graphpad.com/
CellSens	Olympus	https://www.olympus-lifescience.com/en/
Other		
Borosilicate glass	Sutter Instrument	BF150-110-10
Axopatch 200A amplifier	Molecular Devices	https://www.moleculardevices.com
Digidata 1555A digitizer	Molecular Devices	https://www.moleculardevices.com
Multiclamp 700B amplifier	Molecular Devices	https://www.moleculardevices.com
Digidata 1440A digitizer	Molecular Devices	https://www.moleculardevices.com

REAGENT or RESOURCE	SOURCE	IDENTIFIER
CCD camera	The Imaging Source	DMK21AU04.AS
Microscope Eclipse TS-100	Nikon	https://www.nikonmetrology.com/en-us/

Author Manuscript

Author Manuscript

Author Manuscript

Author Manuscript